NASA TN D-1629

TECHNICAL NOTE

D-1629

SURFACE PRESSURE DISTRIBUTIONS INDUCED ON A FLAT PLATE BY A COLD AIR JET ISSUING PERPENDICULARLY FROM THE PLATE AND NORMAL TO A LOW-SPEED FREE-STREAM FLOW

By Raymond D. Vogler

Langley Research Center
Langley Station, Hampton, Va.

NATIONAL AERONAUTICS AND SPACE ADMINISTRATION
WASHINGTON
March 1963

cadet

SINGLE COPY ONLY

NATIONAL AERONAUTICS AND SPACE ADMINISTRATION

TECHNICAL NOTE D-1629

SURFACE PRESSURE DISTRIBUTIONS INDUCED ON A FLAT PLATE BY A COLD AIR JET ISSUING PERPENDICULARLY FROM THE PLATE AND NORMAL TO A LOW-SPEED FREE-STREAM FLOW

By Raymond D. Vogler

SUMMARY

An investigation was made to determine the pressure distribution on the surface of a flat plate induced by a round cold air jet and a rod. Data are presented as pressure-coefficient contours on the plate for various jet and free-stream velocities associated with transition flight speeds of VTOL aircraft.

The jet produces a region of positive pressures upstream of the jet and a larger region of negative pressures laterally and downstream of the jet. This negative pressure field extends 8 or 10 jet diameters from the jet, is intensified by an increase in jet velocity, and is swept downstream by an increase in free-stream velocity.

INTRODUCTION

Many of the proposed VTOL/STOL aircraft have incorporated in their design jet engines or fans for producing lift from the jet reaction. This lifting jet may be from engines set vertically in the fuselage or fans buried in the wing, with the jet issuing from the bottom surface of the aircraft. References 1 to 5 indicate that there is negative lift induced on a wing when a jet issues from the bottom surface of the wing or fuselage in free-stream flow. In the case of VTOL models, force tests of references 2 and 3 show that large nose-up pitching moments occur as a result of jet and free-stream interaction. Some investigations have been made (refs. 4 and 5) to determine pressure distributions on a surface with sonic and supersonic jets exhausting perpendicularly from the surface and normal to a supersonic stream. These results are applicable to missiles and aircraft using small high-speed reaction jets for control, but the results involve speeds far in excess of those pertaining to VTOL aircraft.

The present investigation was made in the Langley 300-MPH 7- by 10-foot tunnel to determine the pressure distributions on the surface of a flat plate with a cold air jet issuing perpendicularly from the plate and normal to a free stream, for velocity ranges that might be encountered in the operation of VTOL aircraft. The jet velocities were approximately 204, 510, and 1,020 feet per second, and

the free-stream velocities ranged from 82 to 408 feet per second. Jet and free-stream velocities were selected to give free-stream to jet-velocity ratios from 0.2 to 1.0. In order to determine any similarity of the flow around the air jet to that around a cylinder, pressure distributions were also taken with a 1-inch-diameter rod replacing the air jet. The combined effects of reducing the plate size and increasing its length-to-width ratio with the jet operating were also investigated.

SYMBOLS

C_p pressure coefficient, $\frac{p - p_\infty}{q_\infty}$

p static pressure on plate, lb/sq ft

p_∞ free-stream static pressure, lb/sq ft

q_∞ free-stream dynamic pressure, lb/sq ft

V free-stream velocity, ft/sec

V_j jet velocity, ft/sec

β angle between orifice rays and longitudinal center line of plate, measured counterclockwise from upstream part of center line, deg

APPARATUS AND PROCEDURE

Dimensions of the plate, orifice locations, nozzle details, and plate location with respect to the tunnel walls are given in figure 1. The plate was held horizontally in the center of the tunnel with a 1.9-inch-diameter pipe which also supplied air to the nozzle. The exit of the 1-inch-diameter converging round nozzle was flush with the plate surface. The orifices were located at intersections of radial lines (rays) and circles concentric with the jet or plate center. (See fig. 1.) With the exception of orifices on rays at 195° and 270°, all orifices were on one side of the plate longitudinal center line.

The rod was simply a cylindrical piece of wood extending from within the round nozzle to the tunnel floor. The small plate was made by cutting away a large part of the original plate.

Pressures at the orifices were recorded by photographing a manometer board which uses alcohol as the fluid. At some of the higher tunnel and jet velocities the manometer height was insufficient to measure the pressure at some orifices near the jet and those pressure tubes were disconnected from the manometer. A total-pressure tube was installed in the 1.9-inch-diameter pipe near the nozzle. The tunnel static pressure and the total pressure inside the nozzle were used for

determining the jet velocity. The method of operation was to set the tunnel velocity and then adjust the total pressure inside the nozzle to give a pressure ratio for the desired nozzle velocity.

ACCURACY

The accuracy of the pressure coefficients, when instrument accuracy and errors in film reading, dynamic-pressure variation, and data fairing are considered, is believed to be within ±0.02. Many scattered points were checked and some groups of points on adjacent orifice rays were checked where the values showed unusual differences between rays. The blockage effect of the air issuing from the nozzle may have produced a small error in the tunnel dynamic pressure reading but such errors would not change the general pattern of a family of pressure-coefficient contours but would produce small changes in the area enclosed within the contours for a given pressure coefficient.

The effect of static-pressure gradient as measured in the clear tunnel is considered negligible. There is a downwash of free-stream flow in the clear tunnel (plate removed) that increases with dynamic pressure and reaches a maximum value of about 0.3° at the highest test dynamic pressure. This misalinement of the plate at the higher tunnel velocities would tend to reduce the static-pressure level over the entire plate. The effect of jet blockage of the free stream on misalinement, if any, is unknown.

RESULTS AND DISCUSSION

General Remarks

Pressures at corresponding orifices on rays at 90° and 270° and at 165° and 195° agreed very closely. The pressure coefficients on the large plate are given in figure 2 for each ray of orifices for the three jet velocities with appropriate free-stream velocities to give a range of ratios of free-stream velocity to jet velocity. Coefficients are given for a radial distance of only 10 inches from the jet center. Beyond this distance there was little variation in coefficient value with distance from the jet center. A small portion of the pressure coefficients at high free-stream and jet velocities may result from a misalinement of the plate with respect to free stream. Positive pressure coefficients upstream ($\beta = 0^\circ$ or $\beta = 30^\circ$) of the jet indicate static pressures on the plate greater than free-stream static pressures. Laterally and downstream of the jet, the pressure coefficients were negative. Negative coefficients as large as -4.0 were obtained very near the jet at the lower ratios of free-stream velocity to jet velocity.

Original plots of the data similar to figure 2 but for the whole plate area were made for the jet and large plate, the jet and small plate, and the rod and large plate. From these original plots the contour lines in figures 3 to 7 were obtained by crossplotting the data for each ray for a selected pressure coefficient for various velocity ratios of each configuration. Some liberty was used

in constructing or neglecting parts of contour lines immediately upstream of the jet where insufficient orifices and mixed flow made locating the exact contour difficult.

Round Air Jet

Large plate.- Pressure-coefficient contours produced by the 1-inch round jet issuing from the large plate are shown in figures 3, 4, and 5. Contours for the entire 24- by 40-inch plate were not plotted, but the central 16- by 20-inch section, represented by the dashed boundary lines on the figures, where the jet effect was greatest is presented. Beyond this region the pressure coefficients were about constant except at the edges, and some of their magnitudes were within the accuracy of the data. The short-dashed curves on the figures show the pressure-coefficient variation with distance from the jet center on the longitudinal center line ($\beta = 0^\circ$ and 180°) of the plate.

The major effect of the jet on the pressure coefficients in the area directly behind the jet occurs within 5 or 6 inches or jet diameters of the jet, but outward and rearward ($\beta = 120^\circ$ and 150°) of the jet exit the affected area may extend for 8 or 10 jet diameters and thus produces a swept lobate form for the contours. This shape results from the deflection of the free stream by the jet and from an expansion and flattening of the jet as it is turned downstream, as may be seen from cross sections of a jet normal to a free stream illustrated in reference 6. The contours of figures 3 to 5 upstream of the jet are fairly uniform in shape but downstream, especially on the center line, the shape of the contours varies with jet and tunnel velocities. This variation in shape may be caused by vortices rolling backward and upward off the edges of the downstream curving jet. The shapes of the contours are similar to those presented in reference 4 except that the downstream contour lobes are swept back less in the present investigation with the low-speed free-stream velocity as compared with the reference data obtained at supersonic speeds.

Although the lift loads on the plate were not integrated from pressures, it is evident from the pressure-coefficient contours that the lift would be negative on the plate region affected by the jet, as was found in the supersonic case reported in reference 5, and the VTOL investigations reported in references 2 and 3. The data also indicate that the positive pressures ahead of and the negative pressures behind the jet would produce large nose-up pitching moments on the plate similar to those shown in references 2 and 3. Swept-wing models would suffer more than unswept-wing models because more of the swept wing would be in the strong negative pressure field.

Small plate.- Some pressure-coefficient contours for the small plate and the 1-inch round jet are presented in figure 6. The boundaries shown represent the actual boundaries of the plate and some of the pressures near the boundaries would be influenced by the edge of the plate, which was not the case with the data presented for the large plate. Except for this edge influence the contours for the small plate are very similar to those of the large plate for coinciding areas and the same free-stream and jet velocities. The strength of the negative

pressure field on the plate increases with jet velocity and the pressure-coefficient contours are usually swept more downstream with an increase in free-stream velocity with either the large or small plate.

Rod

The pressure-coefficient contours and the pressure-coefficient variation along the center line of the large plate with the 1-inch-diameter rod projecting from the plate surface are presented in figure 7 for a range of free-stream velocities. Considering the stated accuracy of the coefficients, the change in free-stream velocity has little effect on the magnitude of the pressure coefficients or contour shape for the plate with the rod. For the highest free-stream velocity (408 feet per second, corresponding to a Reynolds number of 191,000 based on the rod diameter) the pressure coefficients are slightly more negative over most of the plate than for the lower velocities. This is also true for the round jet. Some of this increase in negative coefficient may be the result of plate misalinement caused by the high tunnel velocity. Since there is no expanding jet the lobate form of the contours is less pronounced than that shown with the round jet.

Comparison of Rod and Round-Jet Effects

Figure 8 shows some contours at the same or nearly the same pressure coefficient value taken from previously presented figures to show the relative size, shape, and location of the contours for the round jet and the rod. The rod and jet produce positive pressure fields of about equal area on the plate just upstream of the jet position. The contours of negative pressure coefficient resulting from the round jet generally enclose a larger area and are located farther downstream than those of the rod. These contours would indicate large nose-up pitching moments on the plate that would be increased by the positive pressures on the upstream end of the plate.

CONCLUDING REMARKS

The investigation was made to determine the pressure distribution on the surface of a flat plate with a jet issuing perpendicularly from the plate and normal to the free-stream flow, for velocity ranges that might be encountered in the operation of VTOL aircraft in transition flight. Data were obtained with a large plate with a round nozzle and with a rod replacing the round jet. Some data were also obtained with the round jet blowing from a smaller plate.

The results indicate that a jet issuing from a plate surface produces a region of positive pressures upstream of the jet and a larger region of negative pressures laterally and downstream of the jet. The negative downstream pressure field on the plate is stronger and more extensive than the positive field upstream. The strength of the negative field is appreciable 8 to 10 jet diameters from the jet, and its strength is increased by an increase in jet velocity. The negative pressure field is usually swept farther downstream as the free-stream

velocity is increased. The pressure fields were very similar on the large and the small plates. The pressure field produced on a plate by a cold round jet and that produced by replacing the jet with a rod shows close similarity upstream but differences downstream of the jet.

Langley Research Center,
National Aeronautics and Space Administration,
Langley Station, Hampton, Va., January 11, 1963.

REFERENCES

1. Melbourne, W. H.: Experiments on a Delta Wing With Jet-Assisted Lift. British A.R.C. 21,968, May 31, 1960.

2. Spreemann, Kenneth P.: Investigation of Interference of a Deflected Jet With Free Stream and Ground on Aerodynamic Characteristics of a Semispan Delta-Wing VTOL Model. NASA TN D-915, 1961.

3. Otis, James H., Jr.: Induced Interference Effects on a Four-Jet VTOL Configuration With Various Wing Planforms in the Transition Speed Range. NASA TN D-1400, 1962.

4. Cubbison, Robert W., Anderson, Bernhard H., and Ward, James J.: Surface Pressure Distributions With a Sonic Jet Normal to Adjacent Flat Surfaces at Mach 2.92 to 6.4. NASA TN D-580, 1961.

5. Janos, Joseph J.: Loads Induced on a Flat-Plate Wing by an Air Jet Exhausting Perpendicularly Through the Wing and Normal to a Free-Stream Flow of Mach Number 2.0. NASA TN D-649, 1961.

6. Jordinson, R.: Flow in a Jet Directed Normal to the Wind. R. & M. No. 3074, British A.R.C., 1958.

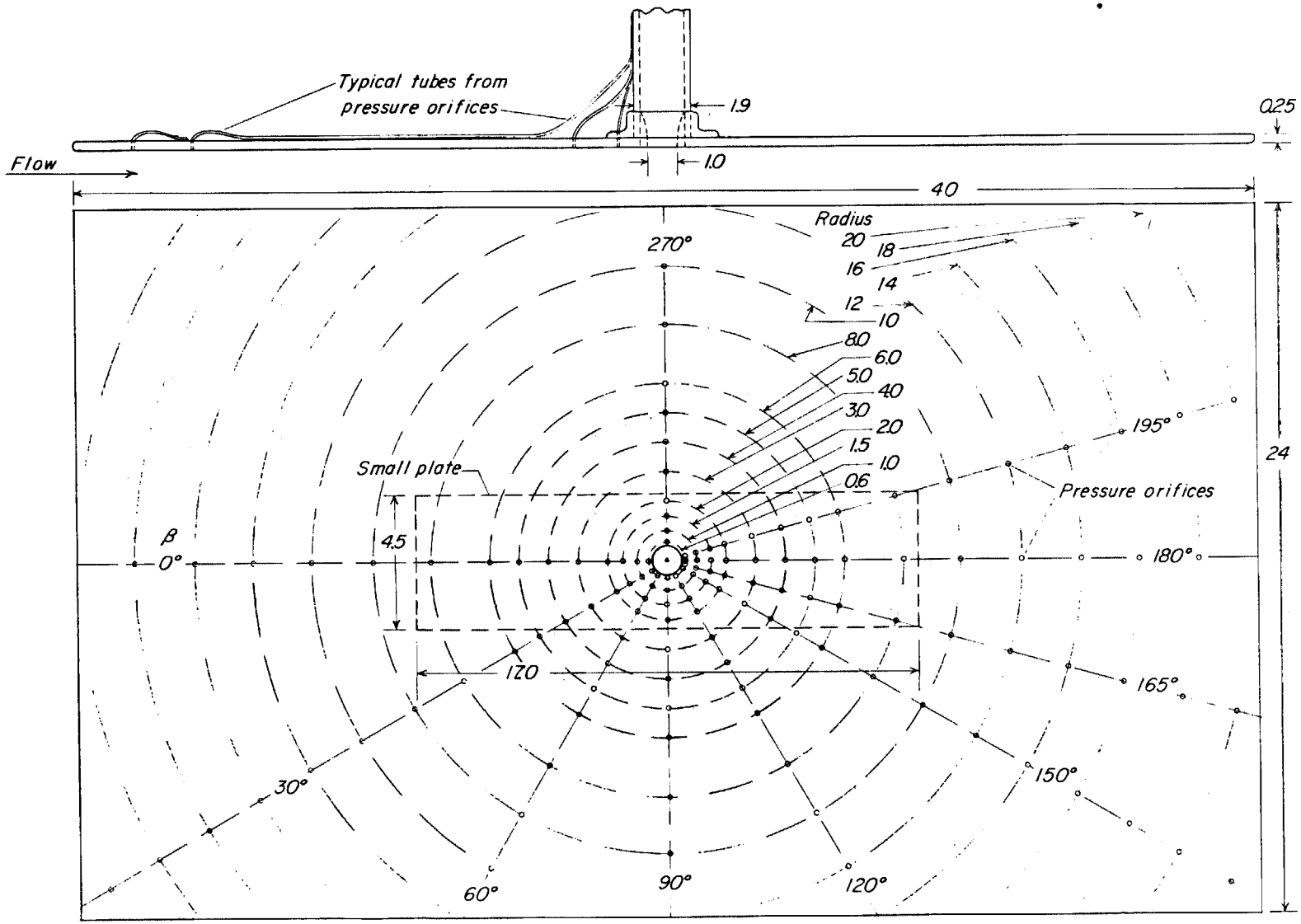

(a) Details of large and small plates and orifice locations.

Figure 1.- Plate location and description. Dimensions are in inches unless otherwise indicated.

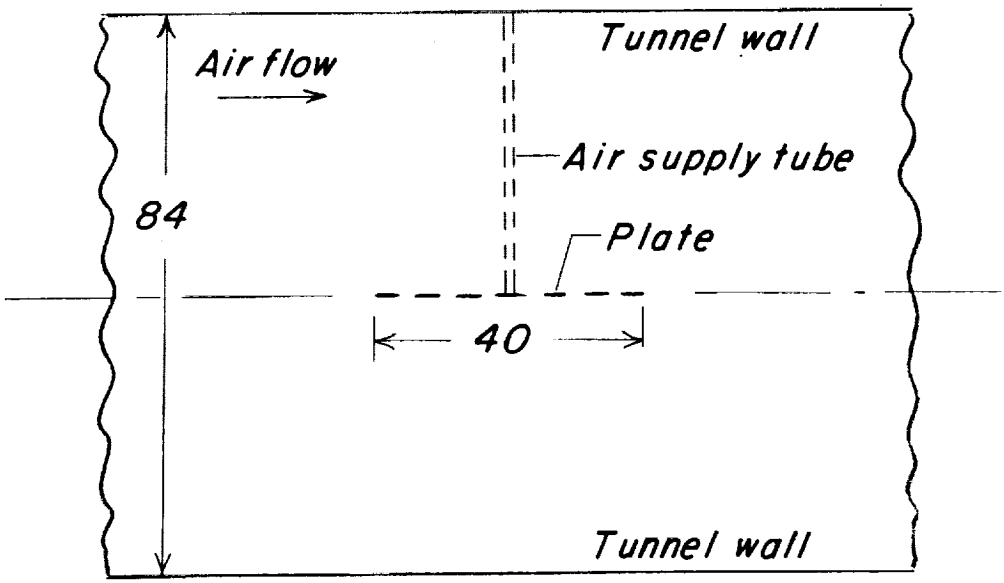

Side view

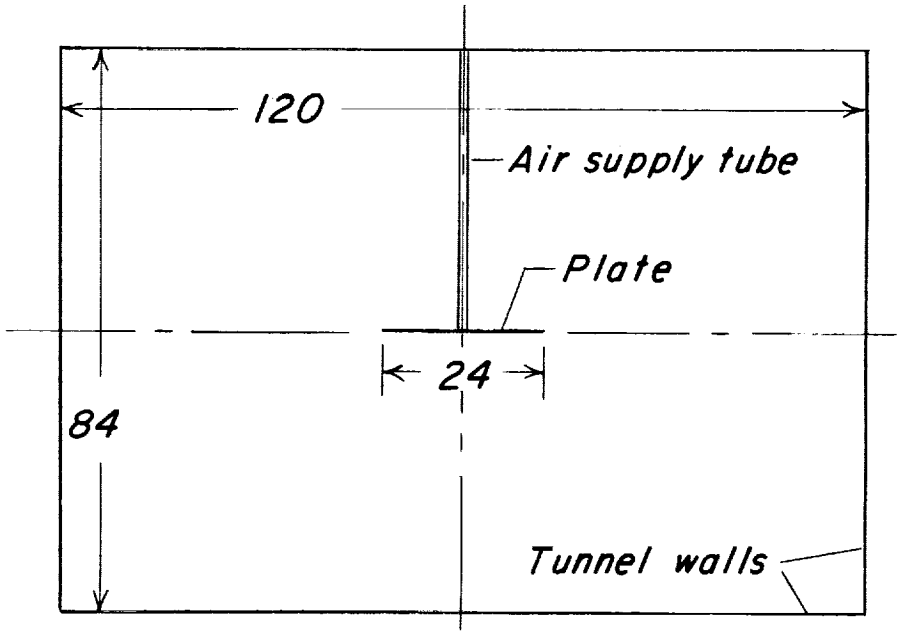

View looking downstream.

(b) Plate location with respect to tunnel walls.

Figure 1.- Concluded.

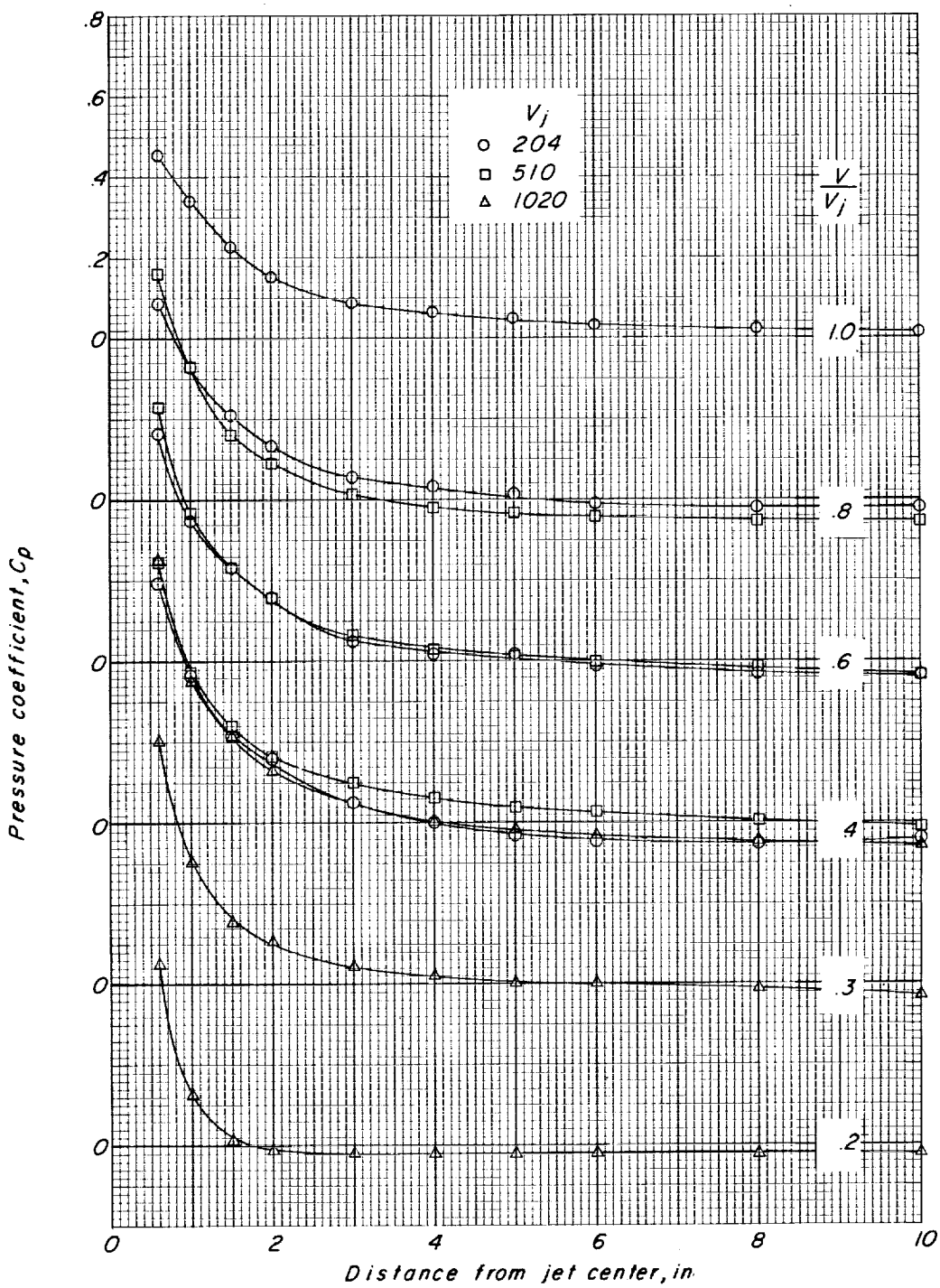

(a) $\beta = 0^{\circ}$.

Figure 2.- Pressure-coefficient variation with distance from the jet center on the large plate for a range of ratios of free-stream velocity to jet velocity.

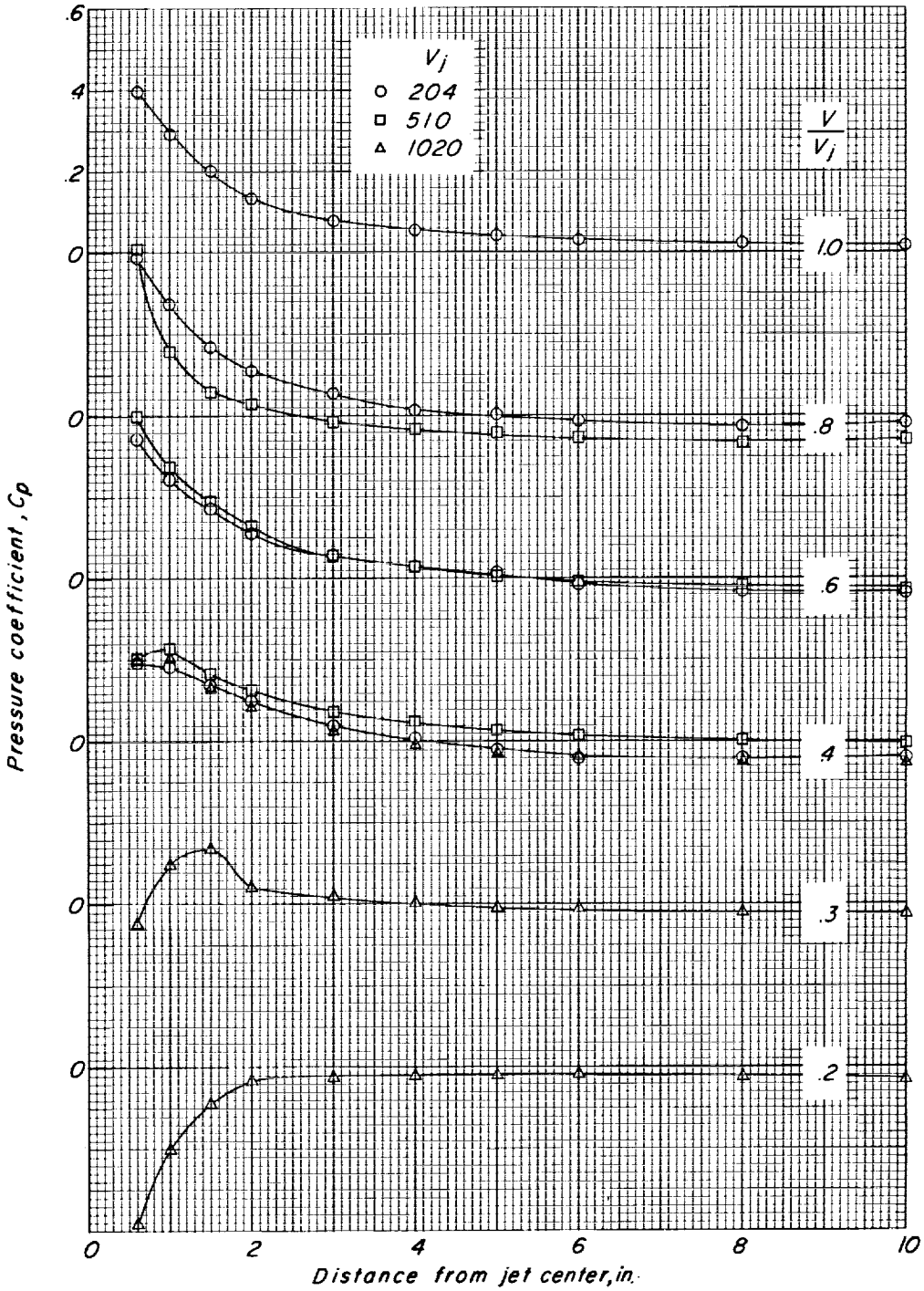

(b) $\beta = 30^{\circ}$.

Figure 2.- Continued.

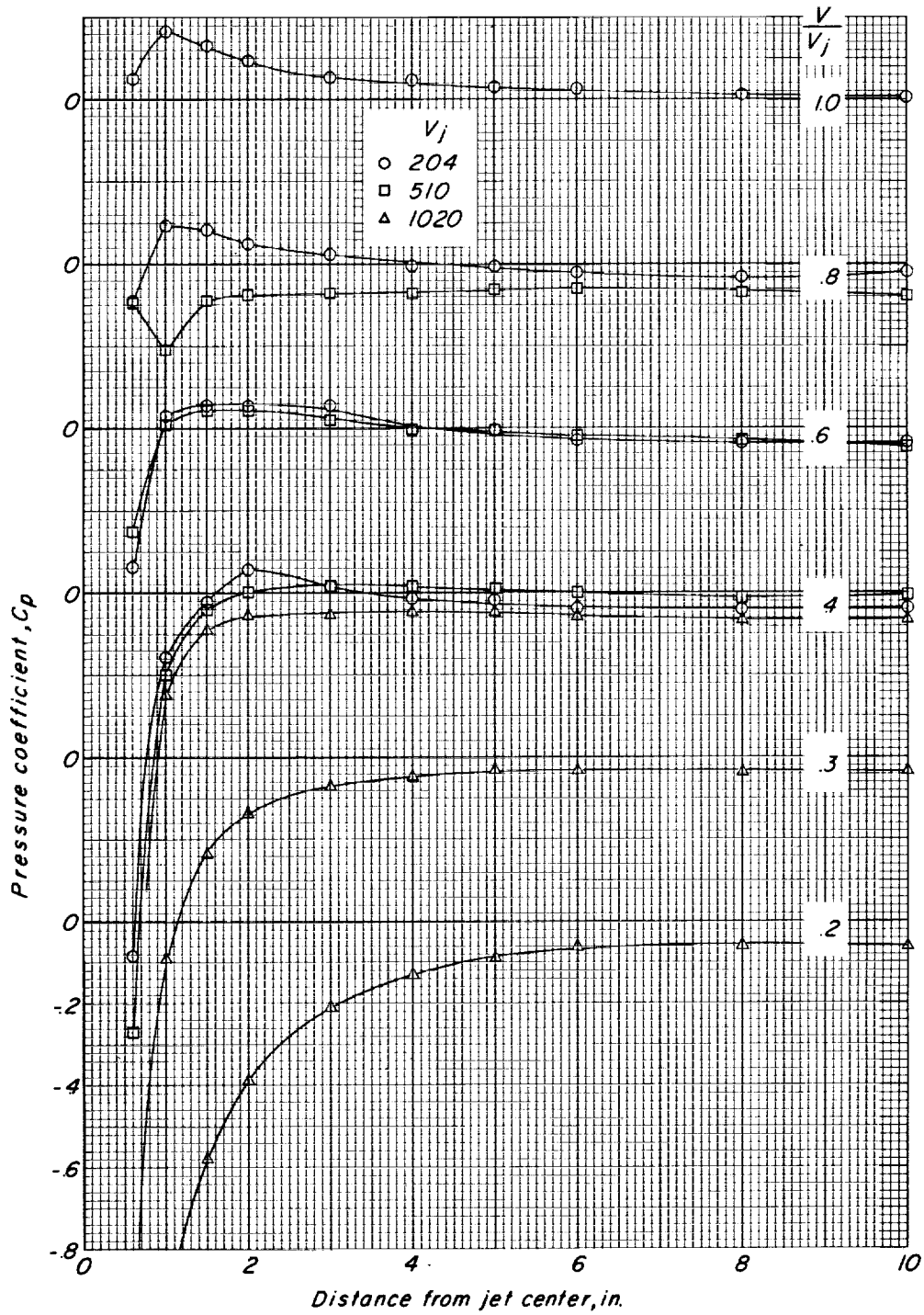

(c) $\beta = 60^{\circ}$.

Figure 2.- Continued.

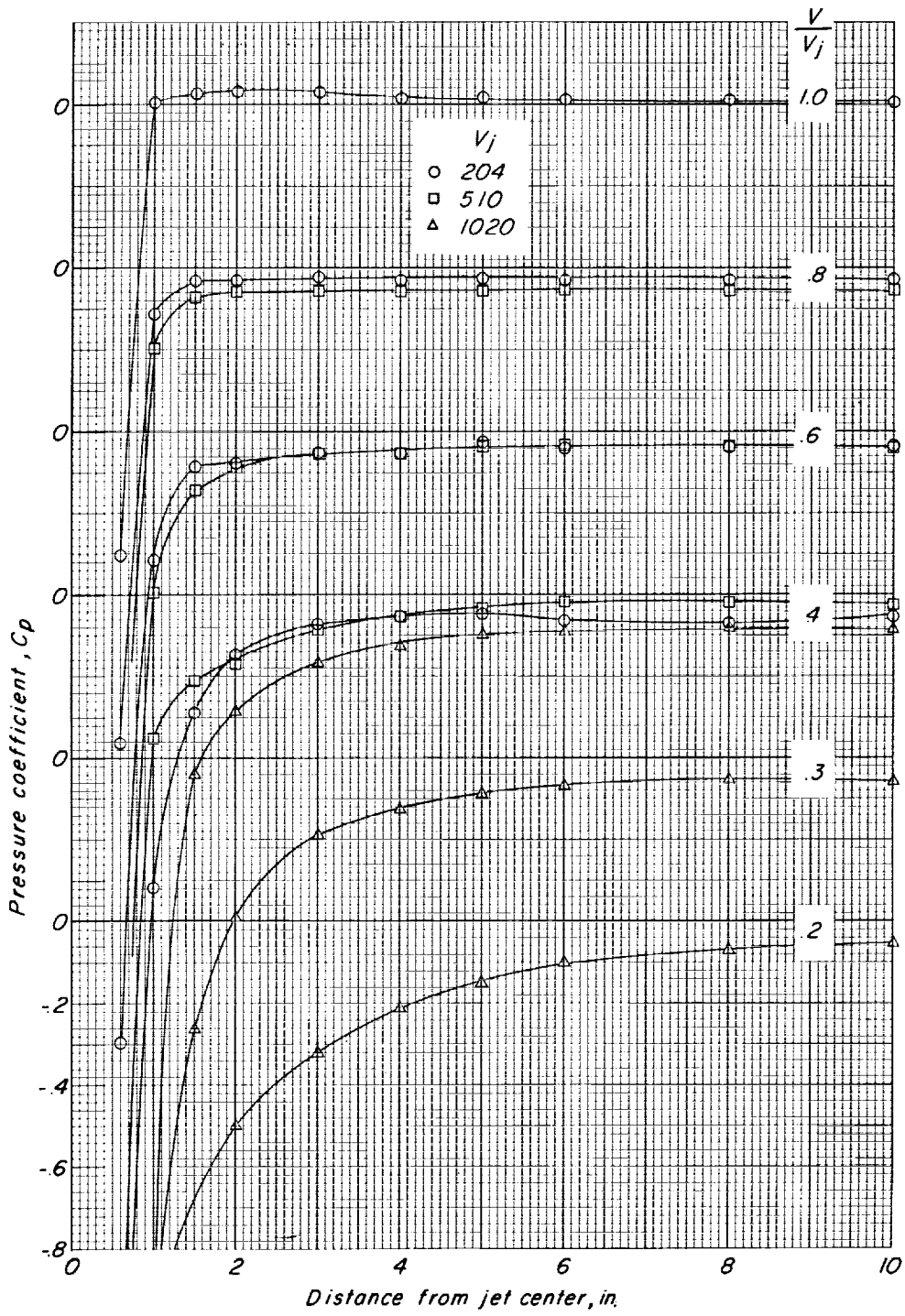

(d) $\beta = 90^{\circ}$.

Figure 2.- Continued.

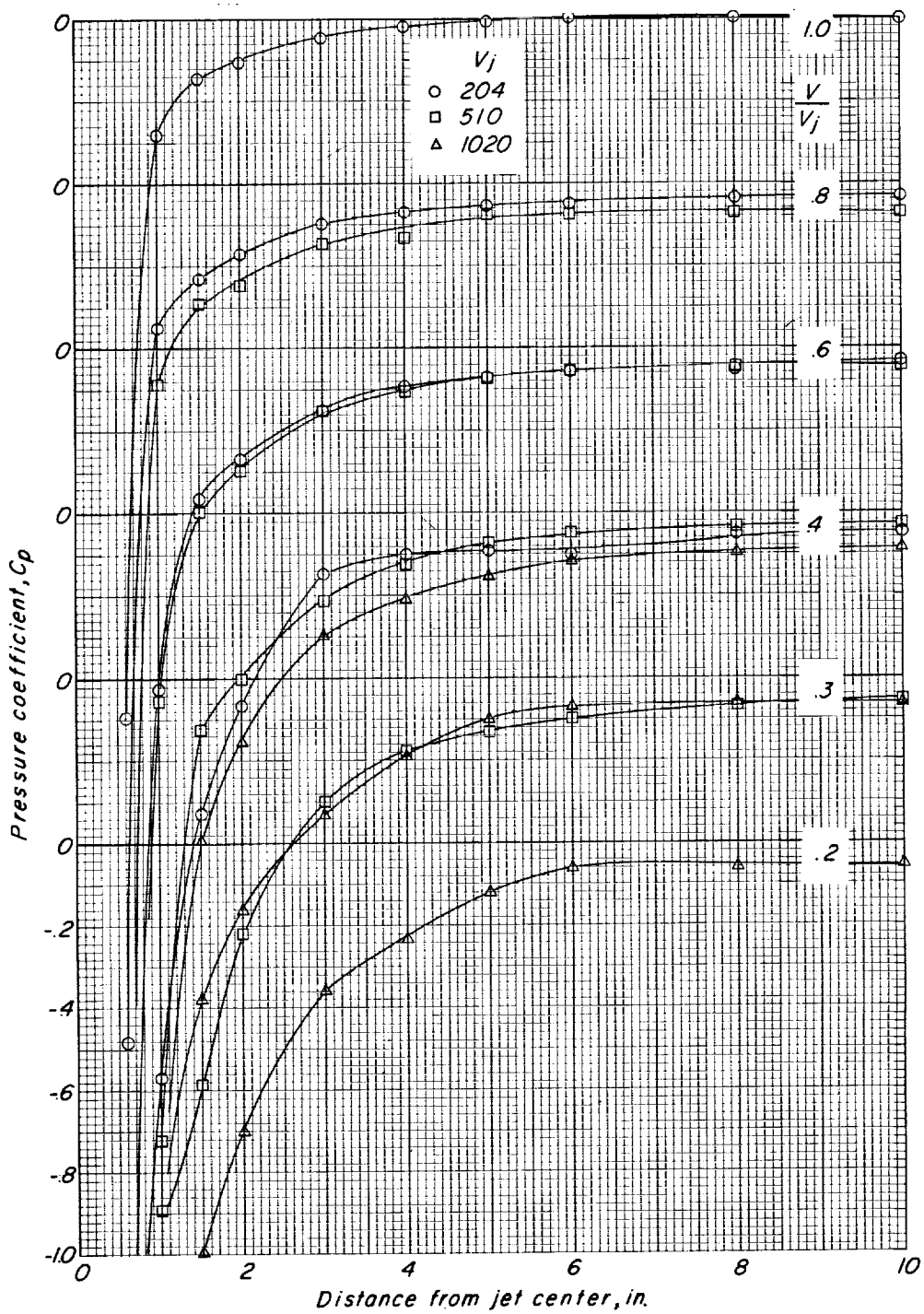

(e) $\beta = 120^{\circ}$.

Figure 2.- Continued.

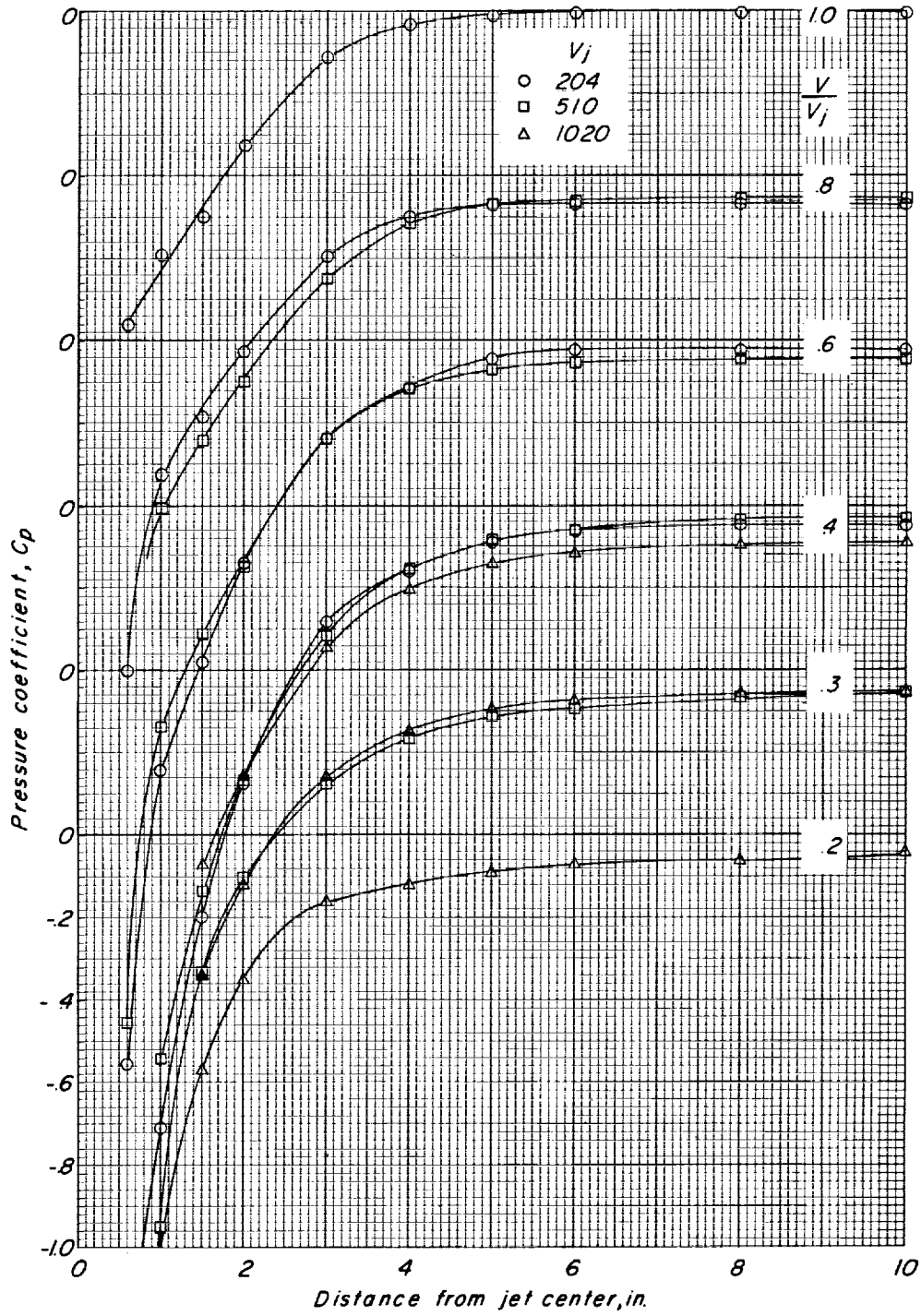

(f) $\beta = 150^{\circ}$.

Figure 2.- Continued.

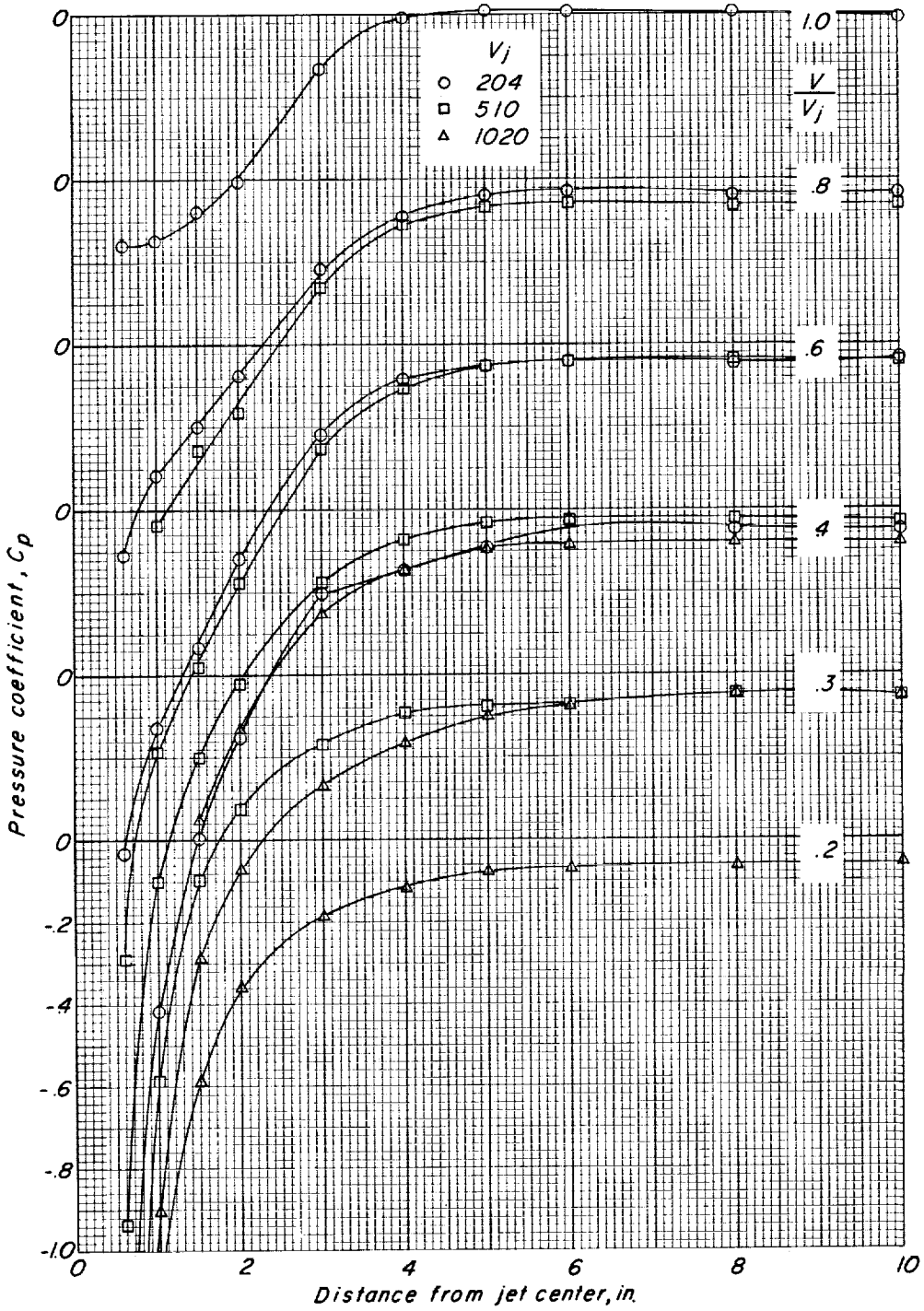

(g) $\beta = 165^{\circ}$.

Figure 2.- Continued.

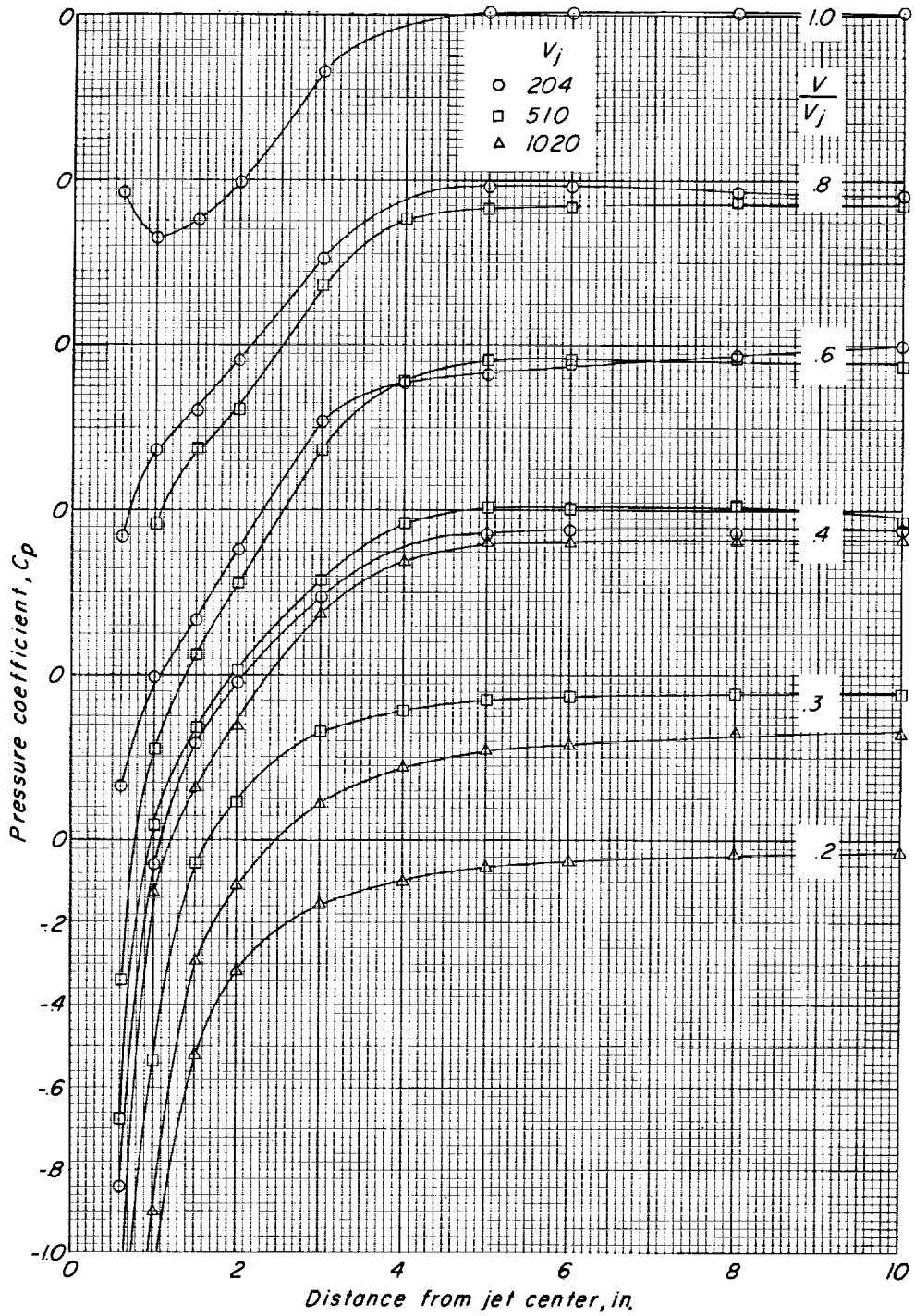

(h) $\beta = 180^{\circ}$.

Figure 2.- Concluded.

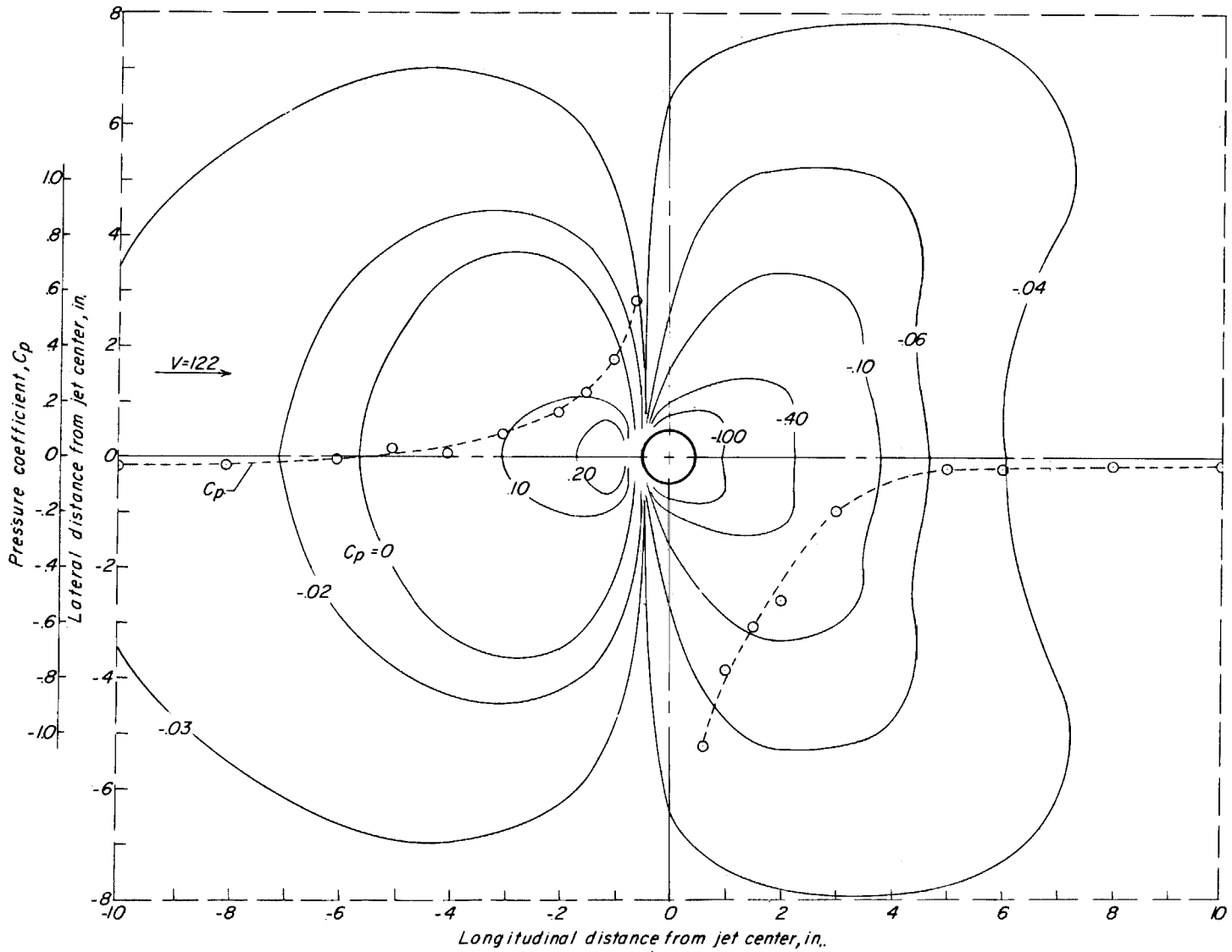

(a) $\frac{V}{V_j} = 0.6$.

Figure 3.- Pressure-coefficient contours on the large plate with the round jet, and pressure-coefficient variation along the longitudinal center line of the plate surface. V_j = 204.

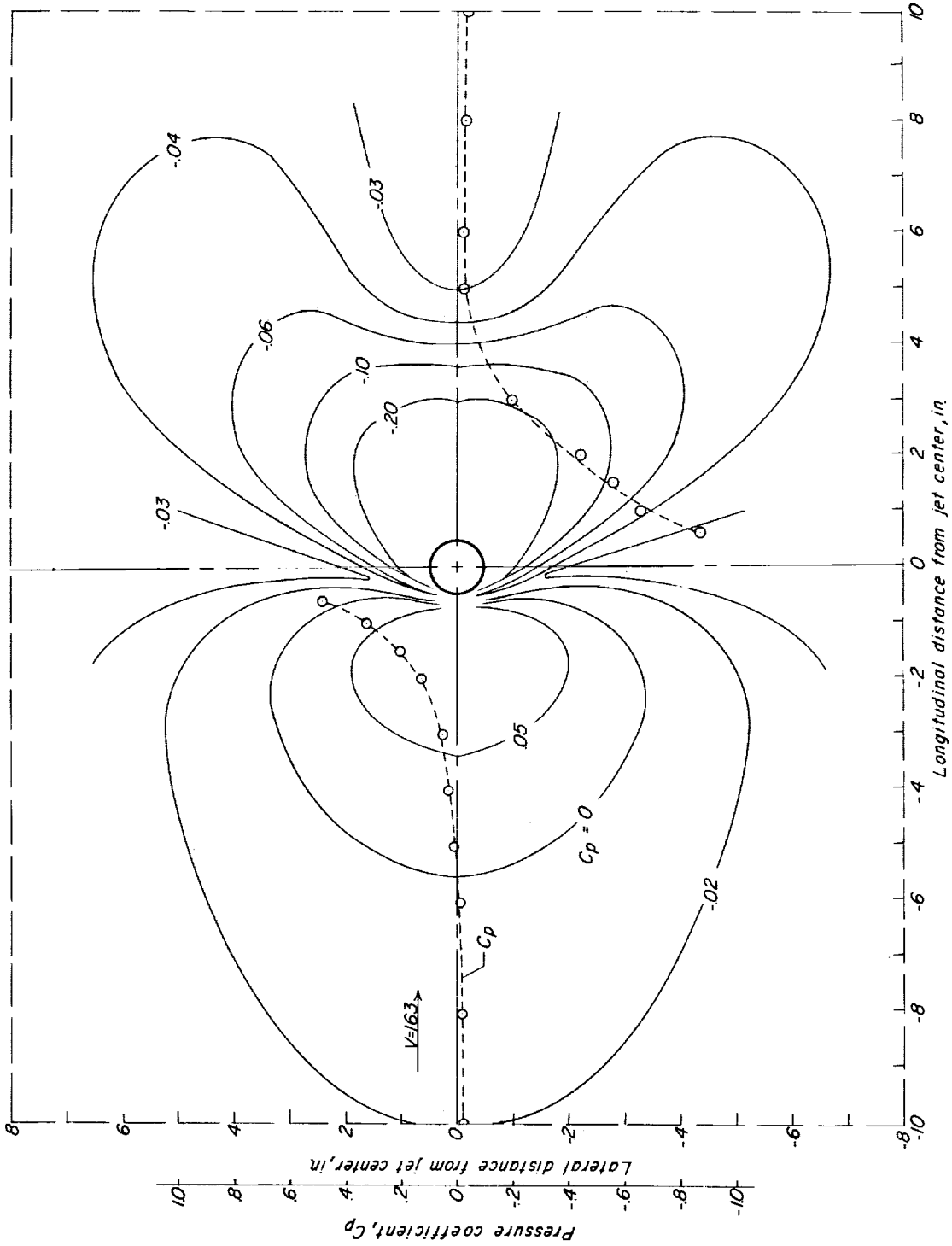

(b) $\frac{V}{V_J} = 0.8$.

Figure 3.- Continued.

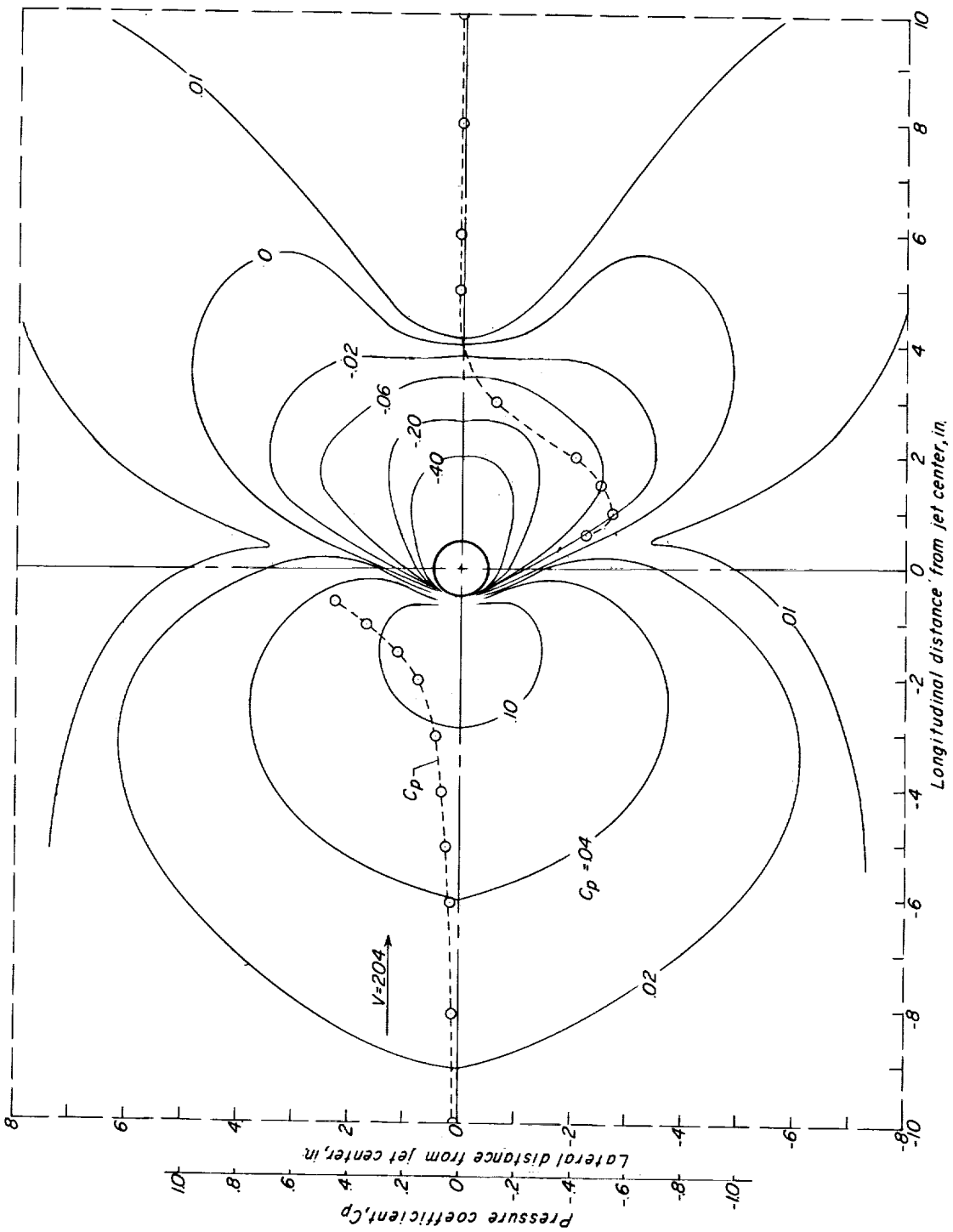

(c) $\frac{V}{V_j} = 1.0$.

Figure 3.- Concluded.

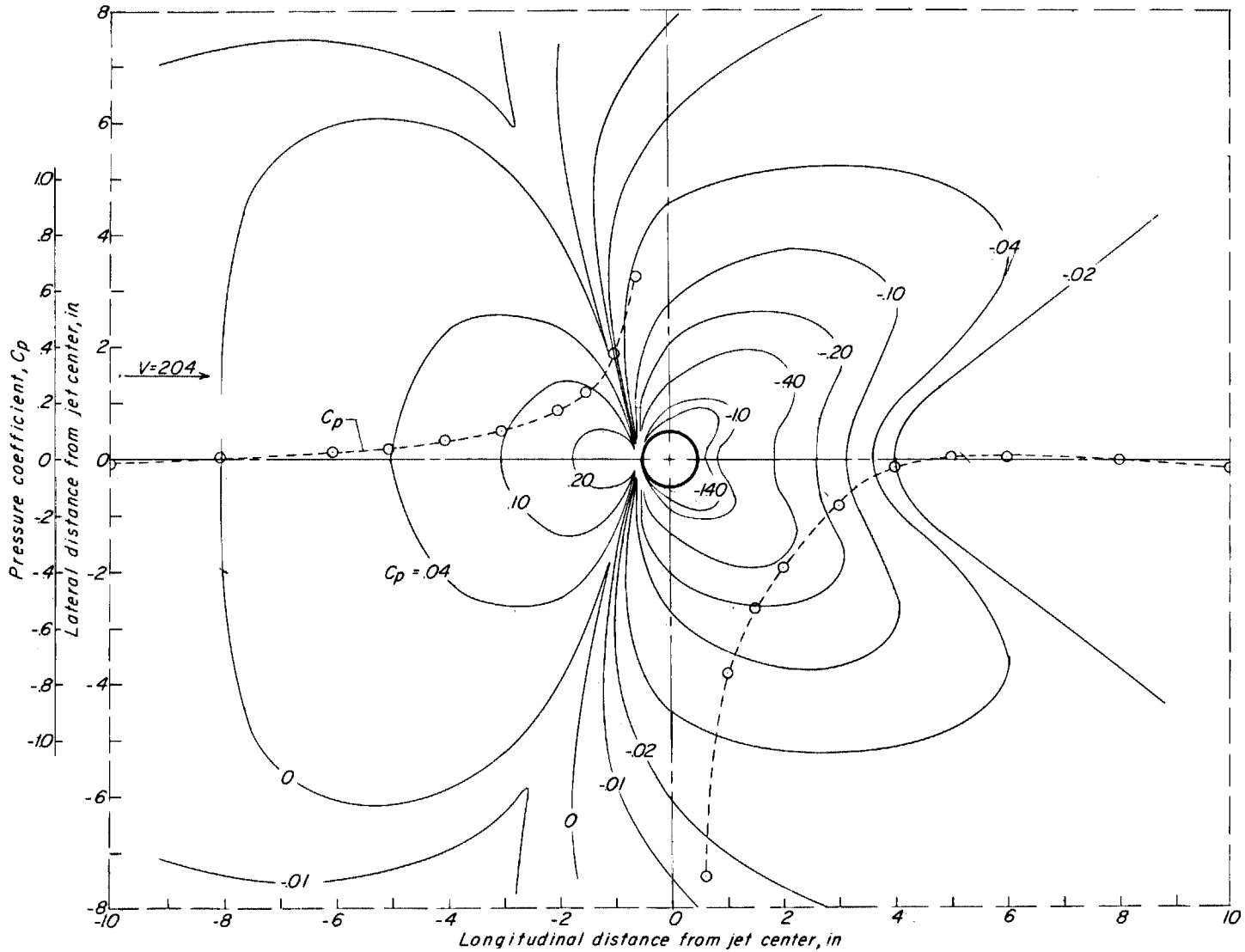

(a) $\frac{V}{V_j} = 0.4$.

Figure 4.- Pressure-coefficient contours on the large plate with the round jet, and pressure-coefficient variation along the longitudinal center line of the plate surface. V_j = 510.

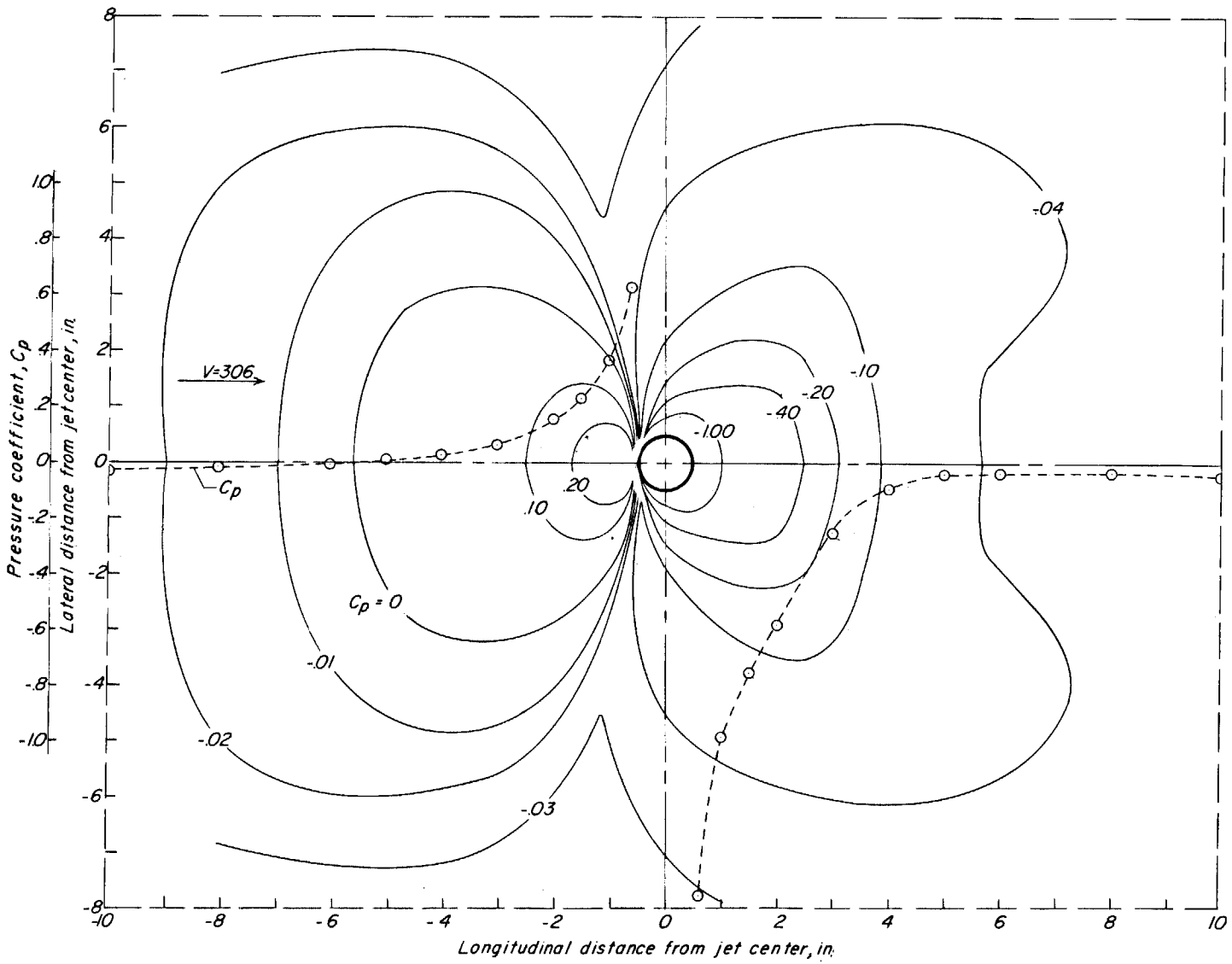

(b) $\frac{V}{V_j} = 0.6$.

Figure 4.- Concluded.

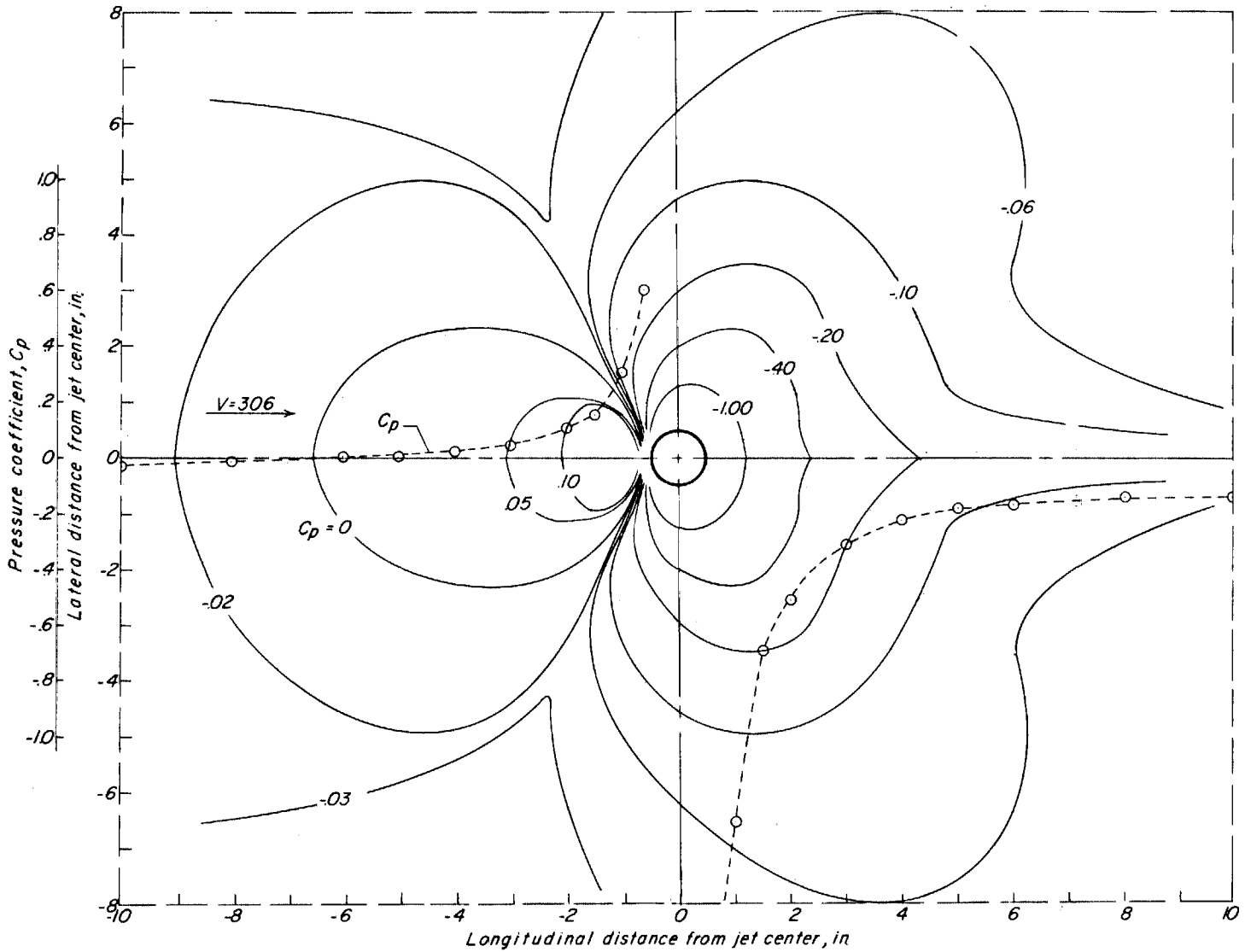

(a) $\frac{V}{V_j} = 0.3$.

Figure 5.- Pressure-coefficient contours on the large plate with the round jet, and pressure-coefficient variation along the longitudinal center line of the plate surface. V_j = 1,020.

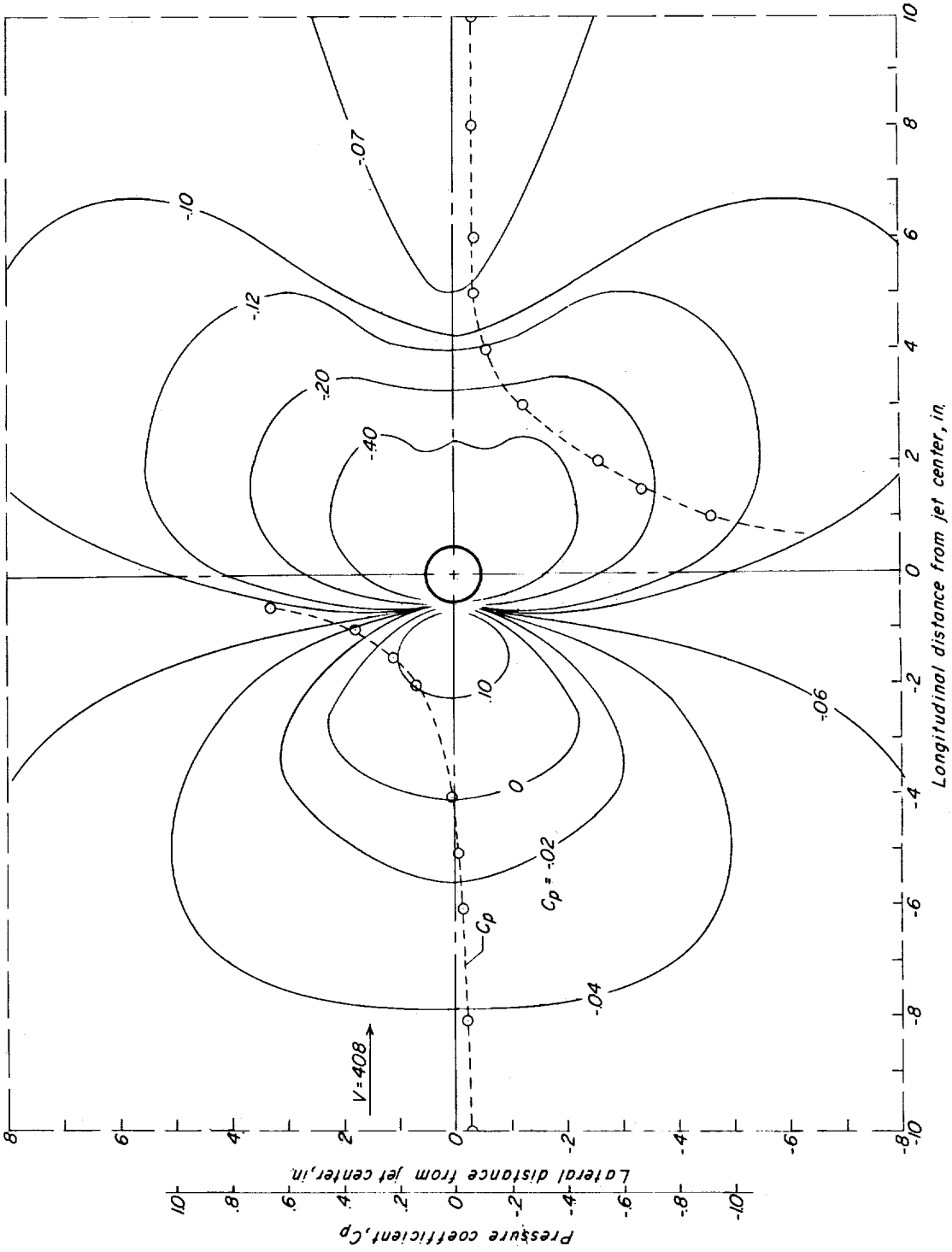

(b) $\frac{V}{V_j} = 0.4$.

Figure 5.- Concluded.

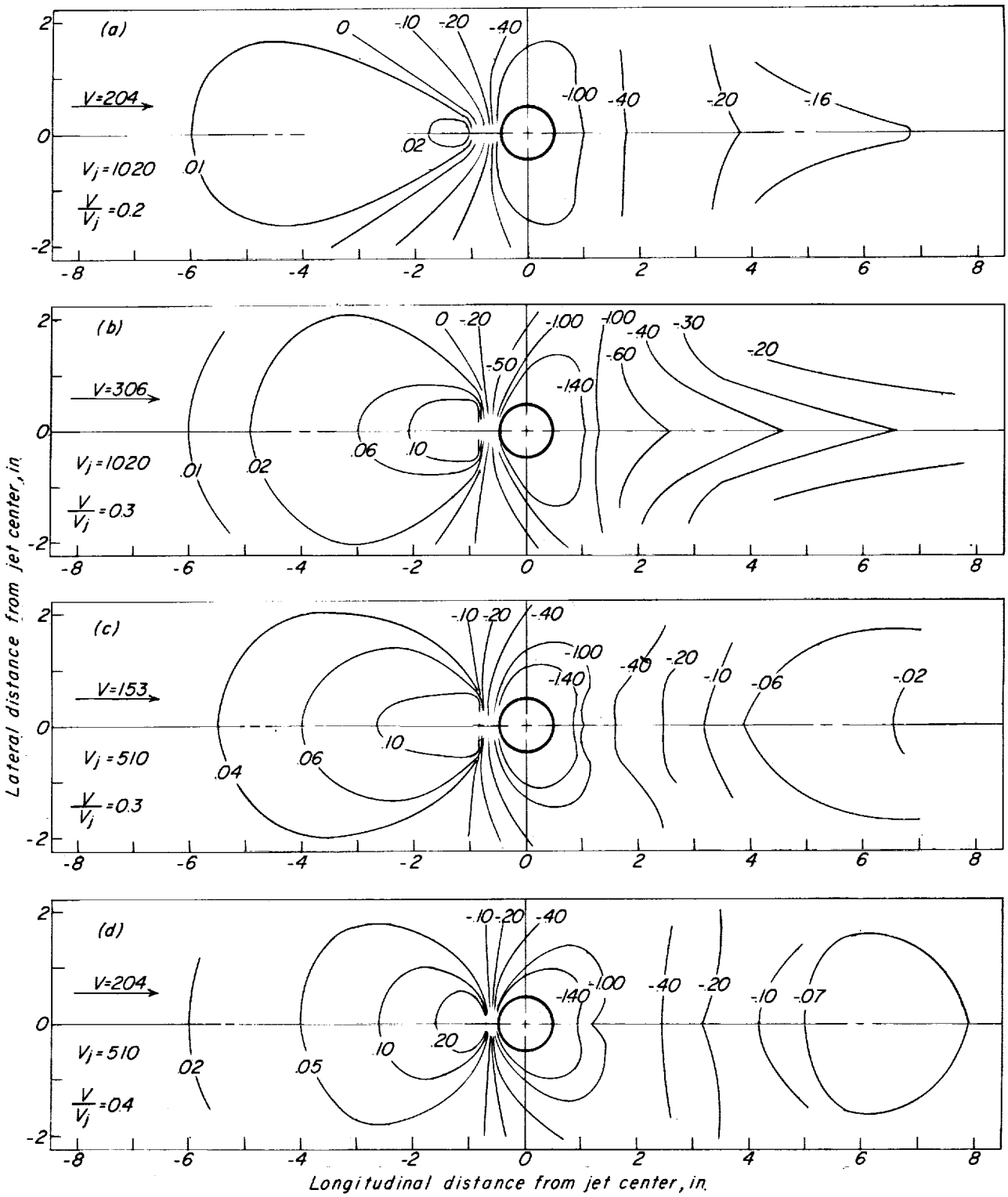

Figure 6.- Pressure-coefficient contours on the small plate with the round jet.

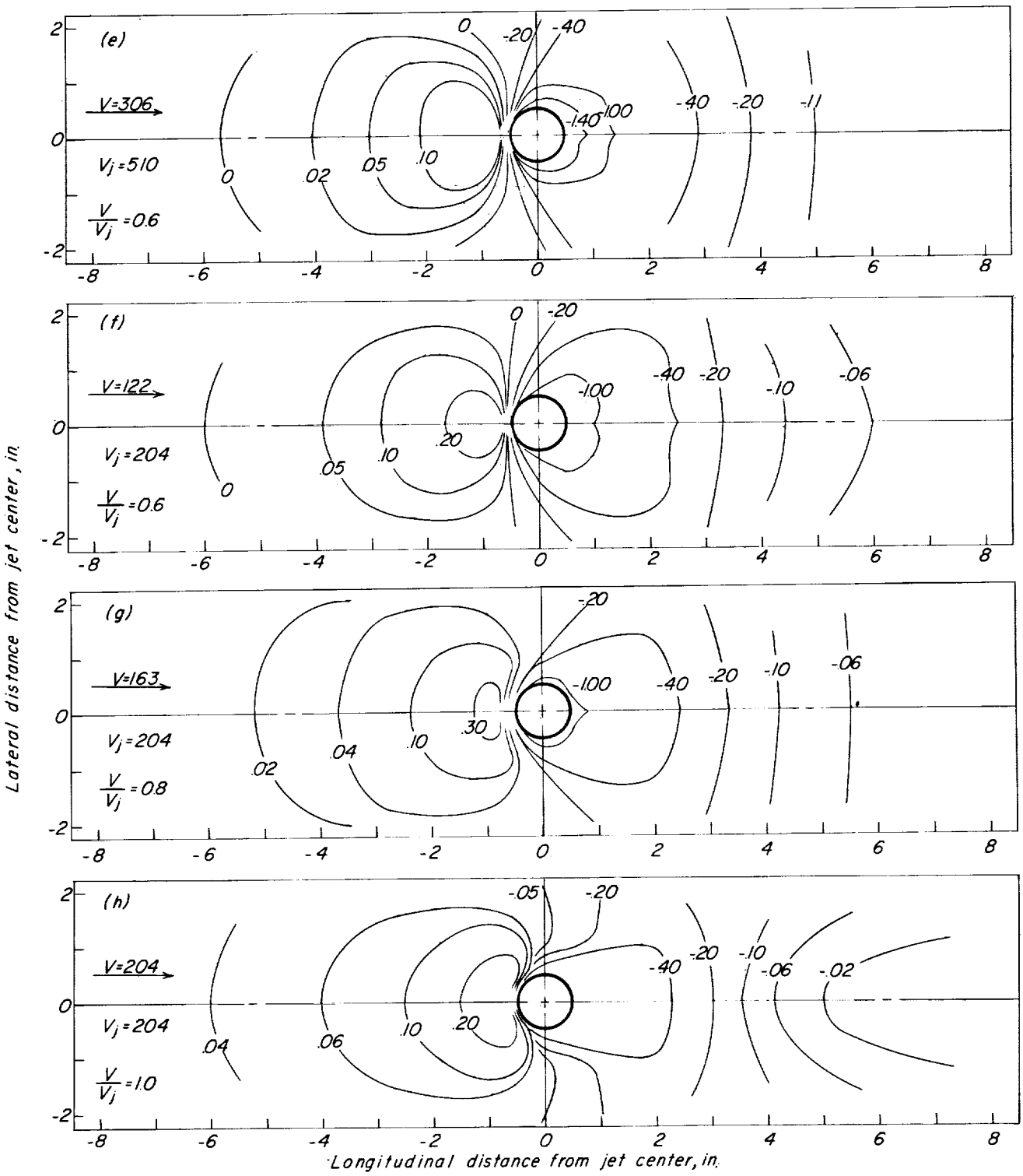

Figure 6.- Concluded.

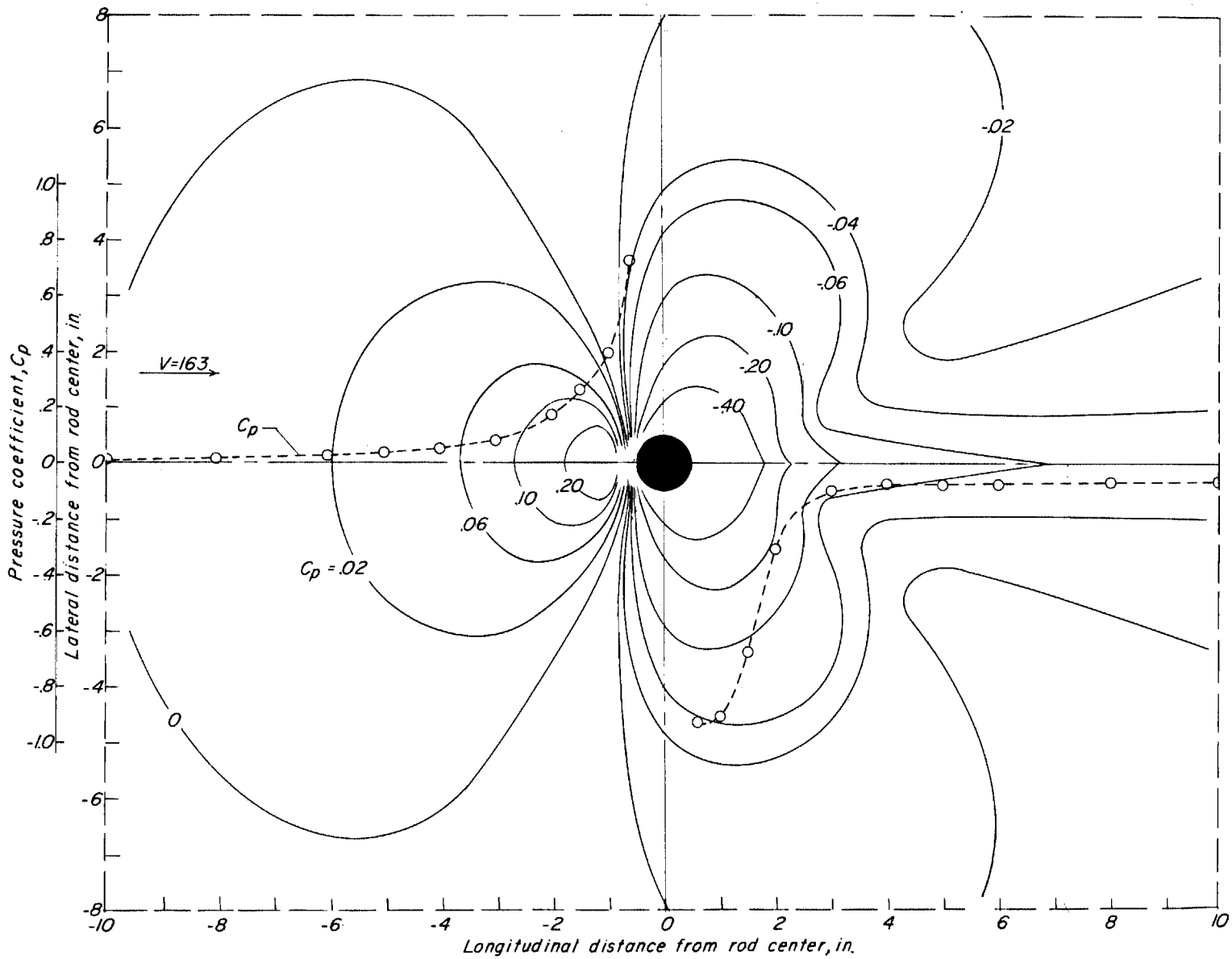

Figure 7.- Pressure-coefficient contours on the large plate with the rod extending from plate to tunnel floor, and pressure-coefficient variation along the longitudinal center line of the plate surface.

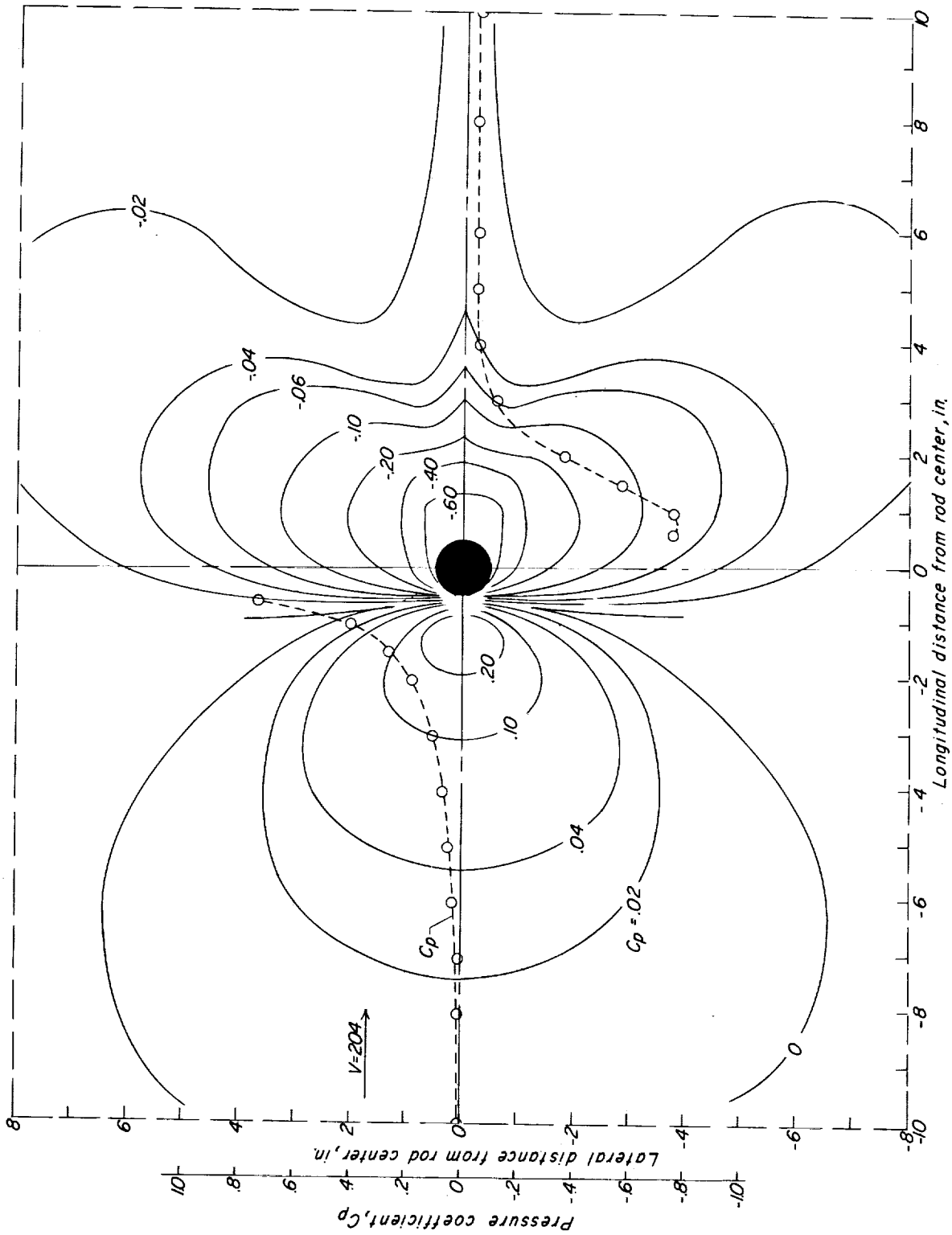

Figure 7.- Continued.

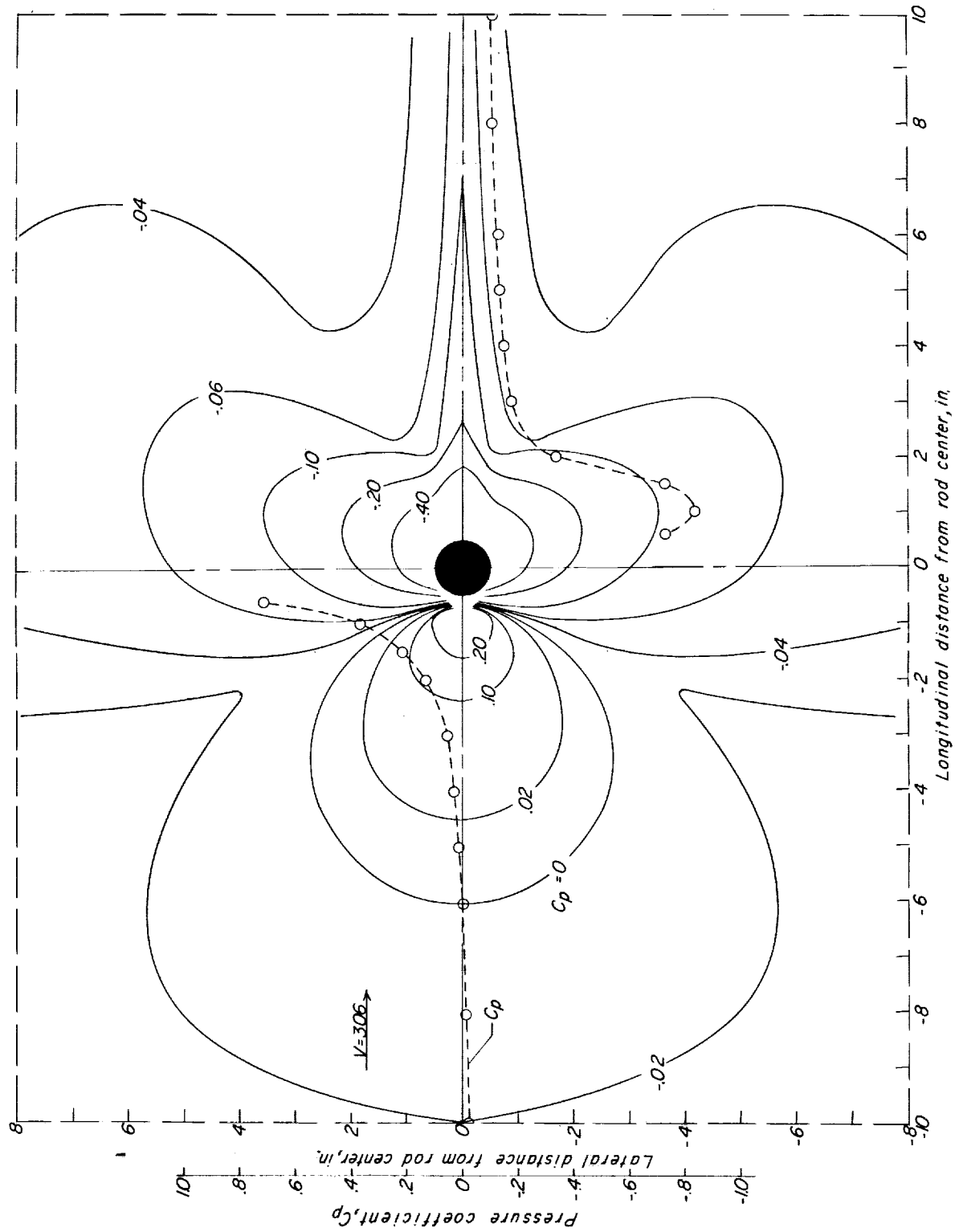

Figure 7.- Continued.

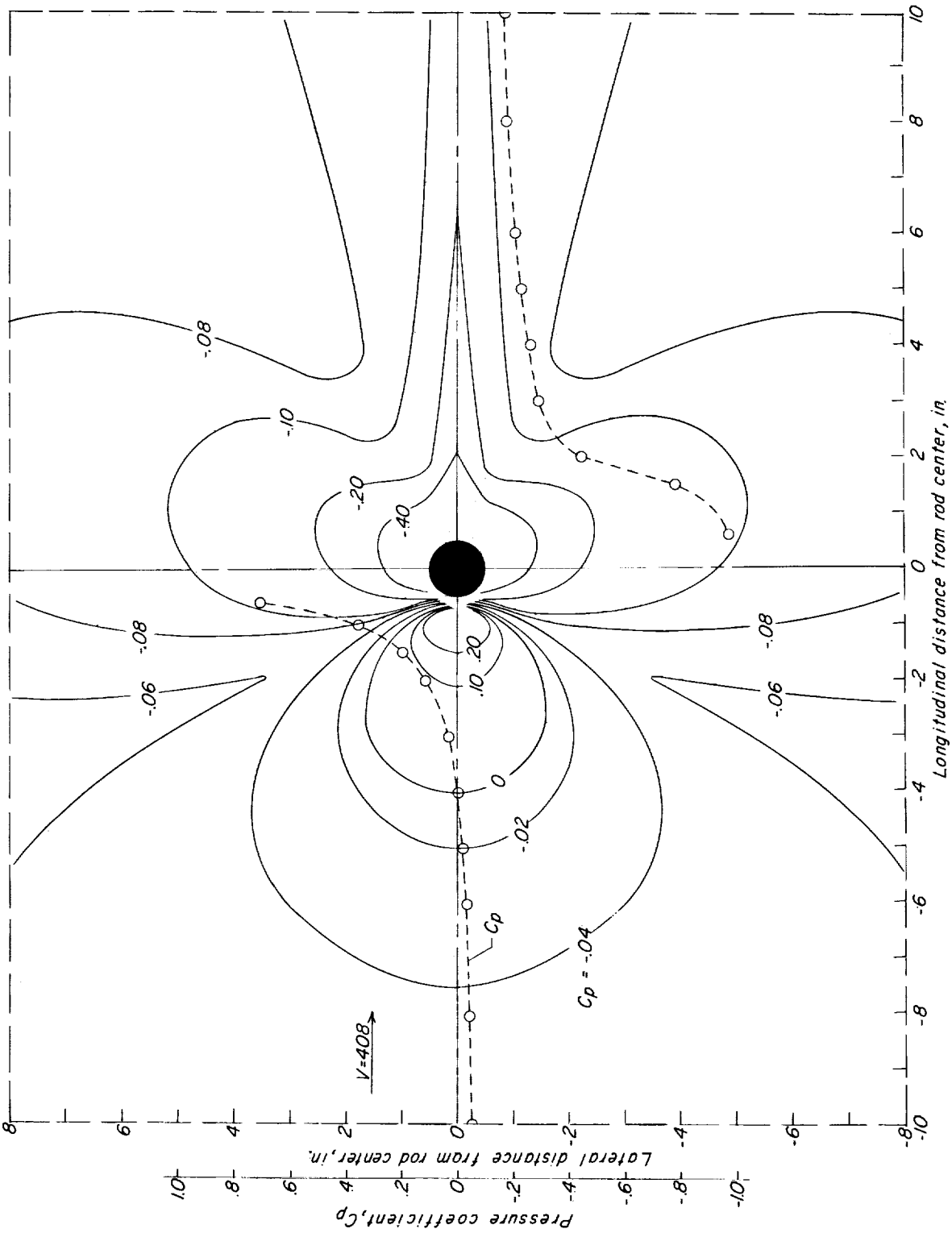

Figure 7.- Concluded.

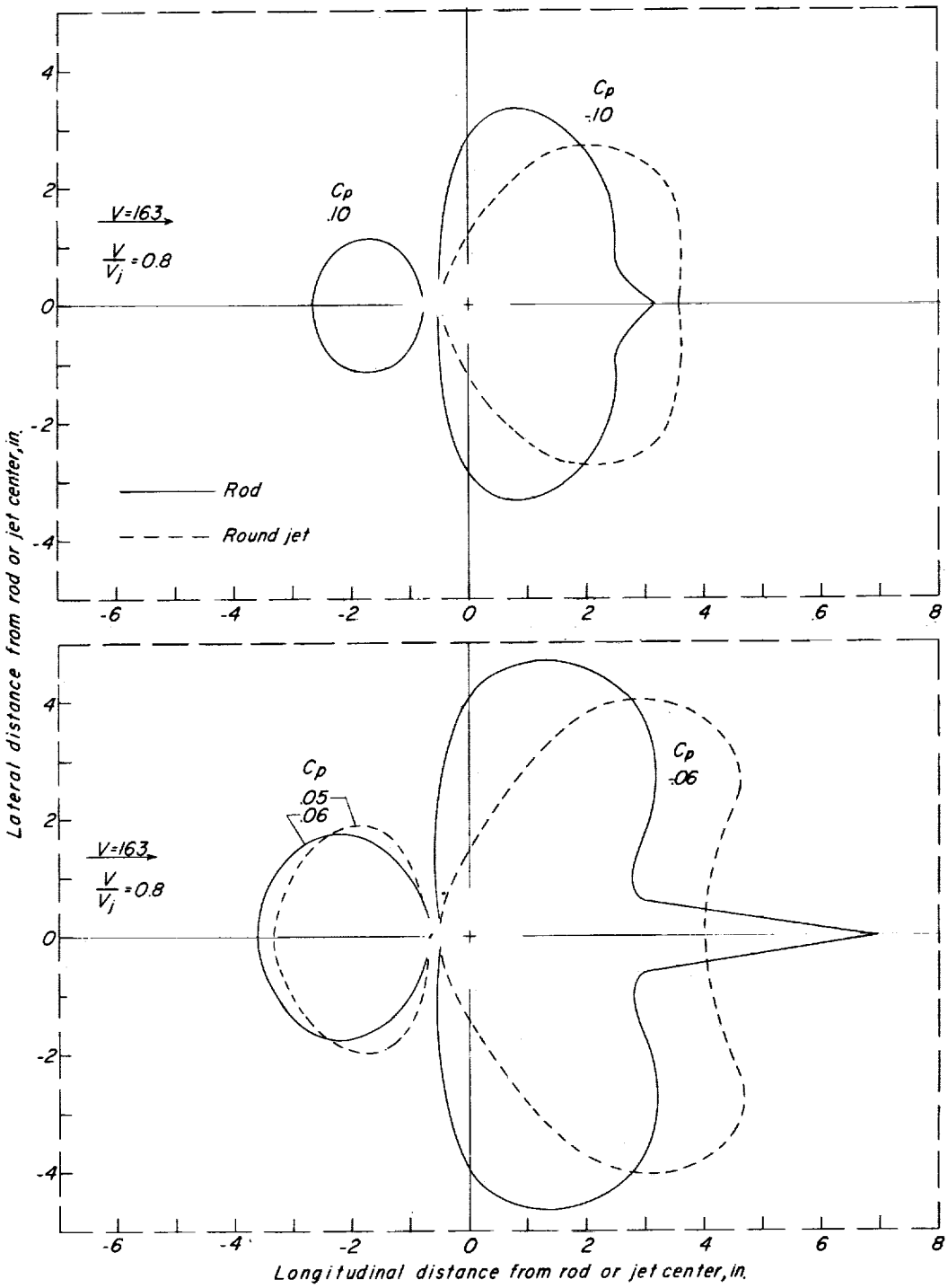

(a) V_j = 204.

Figure 8.- Some comparisons of pressure-coefficient contours on the large plate produced by the rod and the jet for various jet and free-stream velocities.

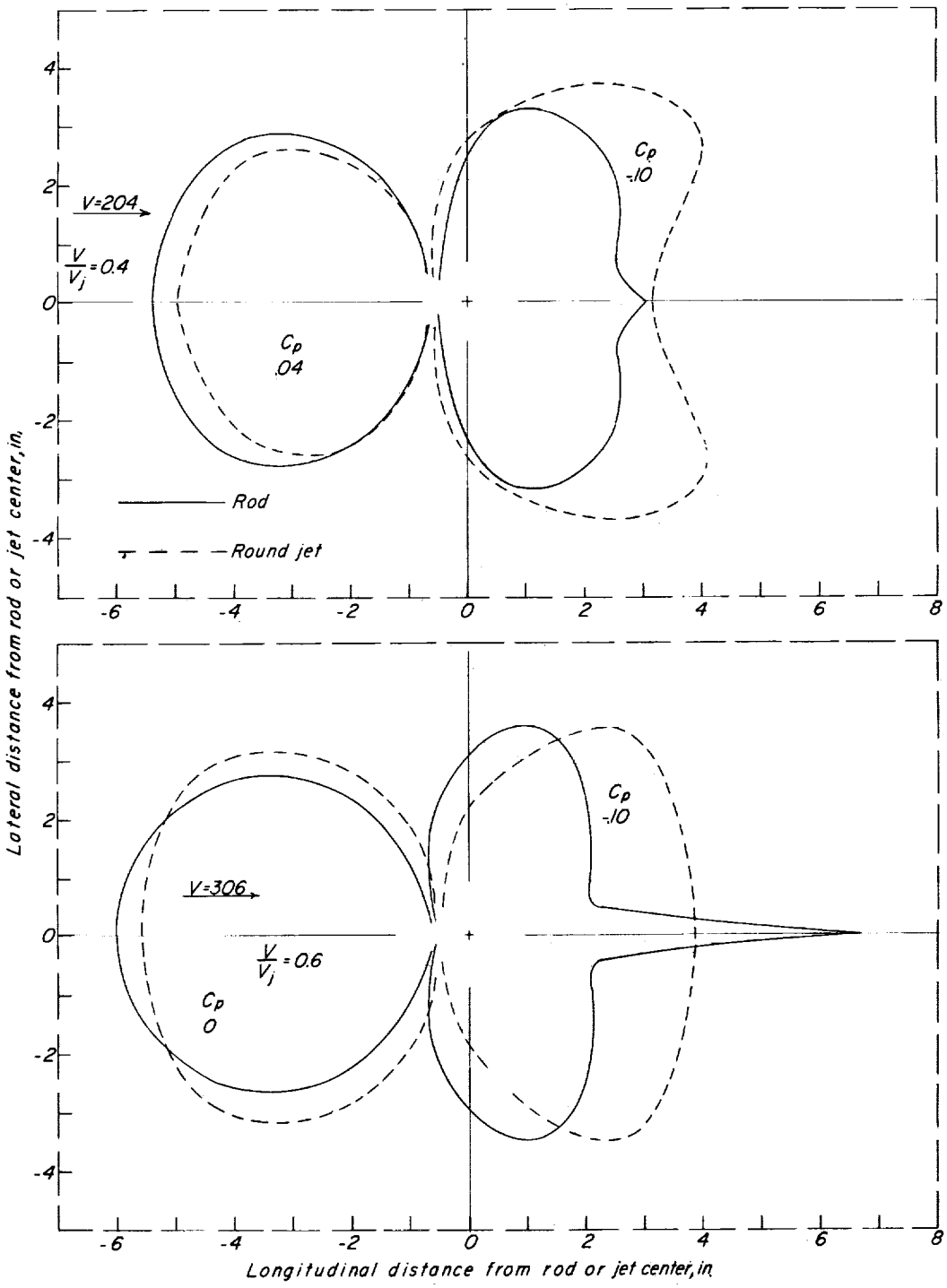

(b) V_j = 510.

Figure 8.- Continued.

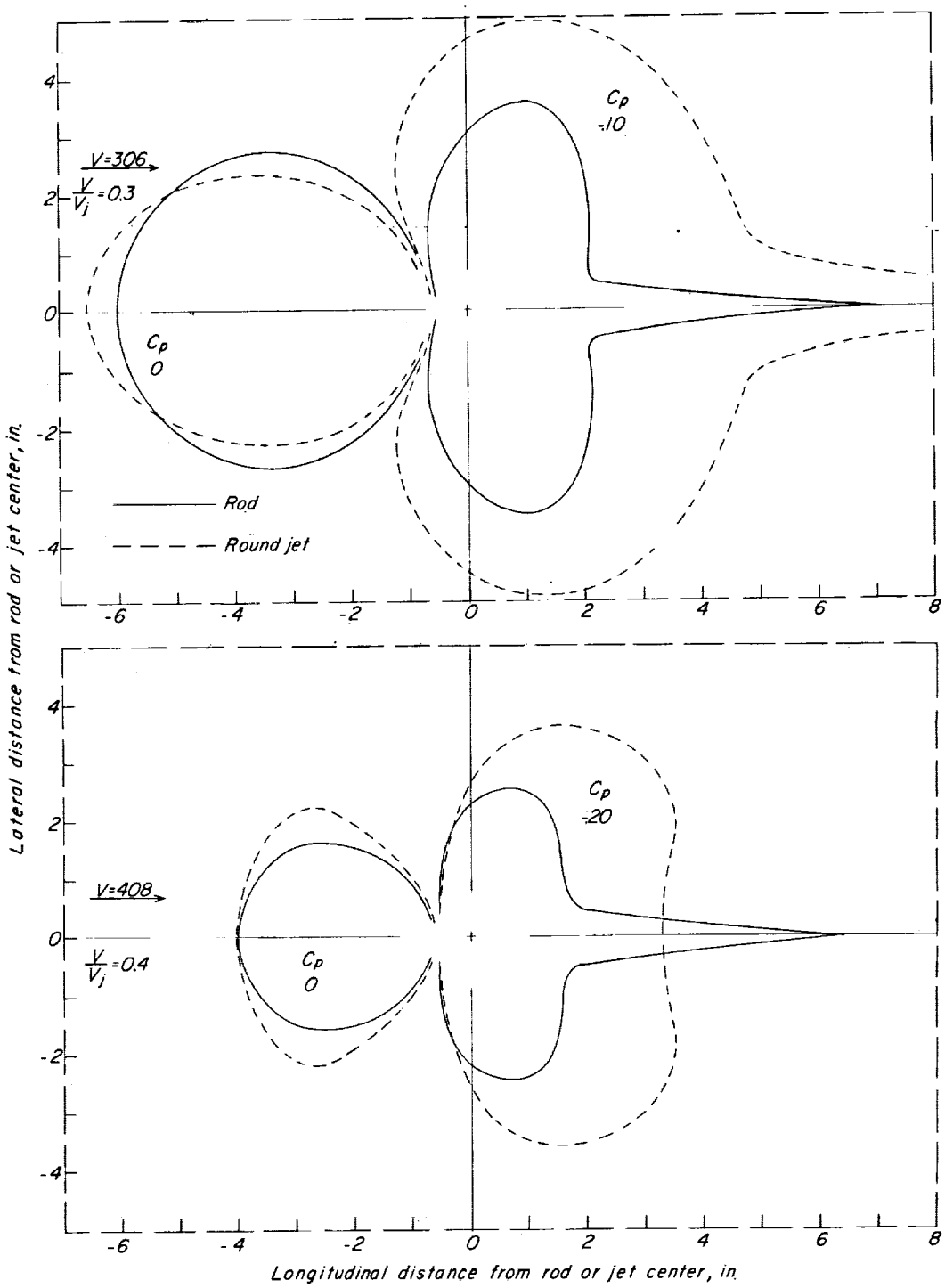

(c) V_j = 1,020.

Figure 8.- Concluded.